The Plant Cell, Vol. 17, 444–463, February 2005, www.plantcell.org © 2005 American Society of Plant Biologists

Functional Genomic Analysis of the *AUXIN RESPONSE FACTOR* Gene Family Members in *Arabidopsis thaliana*: Unique and Overlapping Functions of *ARF7* and *ARF19* [W]

Yoko Okushima,[a,1,2] Paul J. Overvoorde,[a,1,3] Kazunari Arima,[a,4] Jose M. Alonso,[b,5] April Chan,[a] Charlie Chang,[a] Joseph R. Ecker,[b] Beth Hughes,[a] Amy Lui,[a] Diana Nguyen,[a] Courtney Onodera,[a] Hong Quach,[a] Alison Smith,[a] Guixia Yu,[a] and Athanasios Theologis[a,6]

[a] Plant Gene Expression Center, Albany, California 94710
[b] Salk Institute for Biological Studies, La Jolla, California 92037

The AUXIN RESPONSE FACTOR (ARF) gene family products, together with the AUXIN/INDOLE-3-ACETIC ACID proteins, regulate auxin-mediated transcriptional activation/repression. The biological function(s) of most ARFs is poorly understood. Here, we report the identification and characterization of T-DNA insertion lines for 18 of the 23 *ARF* gene family members in *Arabidopsis thaliana*. Most of the lines fail to show an obvious growth phenotype except of the previously identified *arf2/hss*, *arf3/ett*, *arf5/mp*, and *arf7/nph4* mutants, suggesting that there are functional redundancies among the ARF proteins. Subsequently, we generated double mutants. *arf7 arf19* has a strong auxin-related phenotype not observed in the *arf7* and *arf19* single mutants, including severely impaired lateral root formation and abnormal gravitropism in both hypocotyl and root. Global gene expression analysis revealed that auxin-induced gene expression is severely impaired in the *arf7* single and *arf7 arf19* double mutants. For example, the expression of several genes, such as those encoding members of *LATERAL ORGAN BOUNDARIES* domain proteins and *AUXIN-REGULATED GENE INVOLVED IN ORGAN SIZE*, are disrupted in the double mutant. The data suggest that the ARF7 and ARF19 proteins play essential roles in auxin-mediated plant development by regulating both unique and partially overlapping sets of target genes. These observations provide molecular insight into the unique and overlapping functions of *ARF* gene family members in Arabidopsis.

INTRODUCTION

The plant hormone auxin, typified by indole-3-acetic acid (IAA), regulates a variety of physiological processes, including apical dominance, tropic responses, lateral root formation, vascular differentiation, embryo patterning, and shoot elongation (Davies, 1995). At the molecular level, auxin rapidly induces various genes (Abel and Theologis, 1996). Several classes of early auxin-responsive genes have been identified including the *Aux/IAA*, *GH3*, and *SAUR*-like genes (Abel and Theologis, 1996; Guilfoyle et al., 1998). The *GH3*-like genes encode acyl adenylate–forming isozymes (Staswick et al., 2002). Several GH3-like proteins covalently modify IAA, jasmonic acid, or salicylic acid, indicating that they play a global role in various hormone signaling pathways. The function of the *SAUR*-like genes is still unknown, but it has been suggested that they may encode short-lived nuclear proteins involved in auxin signaling by interacting with calmodulin (Yang and Poovaiah, 2000; Knauss et al., 2003).

The *Aux/IAA*s have been among the first auxin-regulated genes to be isolated and are the most characterized among early auxin-responsive genes. They are encoded by a large gene family in *Arabidopsis thaliana* with 29 members (Abel et al., 1995; Reed, 2001; Liscum and Reed, 2002; Remington et al., 2004). They encode short-lived nuclear proteins, and most of them contain four highly conserved domains (I to IV) (Abel et al., 1994; Reed, 2001). Each domain contributes to the functional properties of the protein. Domain II confers instability of the protein (Worley et al., 2000; Ouellet et al., 2001). Domains III and IV serve for homodimerization and heterodimerization with other *Aux/IAA* gene family members as well as for heterodimerization with the Auxin Response Factors (ARFs) (Kim et al., 1997; Ulmasov et al., 1997, 1999a, 1999b). Domain I is responsible for the transcriptional repressing activity of the proteins (Tiwari et al., 2004).

The ARF proteins are also encoded by a large gene family in Arabidopsis (23 members). A typical ARF protein contains a B3-like DNA binding domain in the N-terminal region, and domains III and IV are similar to those found in the C terminus of Aux/IAAs. An ARF binds to auxin-responsive *cis*-acting elements (*AuxREs*) found in the promoter region of auxin-responsive genes through

[1] These authors contributed equally to this work.
[2] Current address: Nara Institute of Science and Technology, Takayama 8916-5, Ikoma, Nara 630-0101, Japan.
[3] Current address: Macalester College, St. Paul, MN 55105.
[4] Current address: Department of Chemistry and BioScience, Faculty of Science, Kagoshima University, Kagoshima 890-0065, Japan.
[5] Current address: Department of Genetics, North Carolina State University, Raleigh, NC 27695.
[6] To whom correspondence should be addressed. E-mail theo@nature.berkeley.edu; fax 510-559-5678.
The author responsible for distribution of materials integral to the findings presented in this article in accordance with the policy described in the Instructions for Authors (www.plantcell.org) is: Athanasios Theologis (theo@nature.berkeley.edu).
[W] Online version contains Web-only data.
Article, publication date, and citation information can be found at www.plantcell.org/cgi/doi/10.1105/tpc.104.028316.

its DNA binding domain (Abel et al., 1996; Ulmasov et al., 1997, 1999a). The amino acid composition of the middle region between the DNA binding domain and domains III/IV determines whether an ARF protein functions as an activator or repressor (Ulmasov et al., 1999b; Tiwari et al., 2003). The Aux/IAA proteins regulate auxin-gene expression through interaction with the ARF proteins. The Aux/IAAs are targets for degradation by the SCF^{TIR1} complex, and most importantly, auxin mediates their interaction with the proteolytic machinery (Gray et al., 1999, 2001; Ward and Estelle, 2001; Dharmasiri and Estelle, 2004). Aux/IAA protein stability is a central regulator in auxin signaling.

Several gain-of-function Aux/IAA mutants, including *shy2/iaa3* (Tian and Reed, 1999), *axr2/iaa7* (Nagpal et al., 2000), *bdl/iaa12* (Hamann et al., 2002), *slr/iaa14* (Fukaki et al., 2002), *arx3/iaa17* (Rouse et al., 1998), *msg2/iaa19* (Tatematsu et al., 2004), and *iaa28-1* (Rogg et al., 2001), have been isolated by forward genetics. These mutants have amino acid substitutions in highly conserved residues of domain II, resulting in enhanced protein stability that causes altered auxin response and dramatic defects in growth and development. Loss-of-function mutations of *AUX/IAA*s do not show an obvious visible growth phenotype (Rouse et al., 1998; Tian and Reed, 1999; Nagpal et al., 2000; P.J. Overvoorde and Y. Okushima, unpublished data). Loss-of-function mutants in five *ARF* genes have been previously isolated. Mutations in the *ARF3/ETT* affect gynoecium patterning (Sessions et al., 1997; Nemhauser et al., 2000). Loss-of-function mutations of *ARF7/NPH4/MSG1/TIR5* result in impaired hypocotyl response to blue light and other differential growth responses associated with changes in auxin sensitivity (Watahiki and Yamamoto, 1997; Stowe-Evans et al., 1998; Harper et al., 2000). Mutations in *ARF5/MP* interfere with the formation of vascular strands and the initiation of the body axis in the early embryo (Hardtke and Berleth, 1998). Mutations in *ARF2/HSS* have been identified as suppressors of the hookless phenotype (Li et al., 2004). *ARF2* acts as a communication link between the ethylene and the auxin signaling pathways for regulating hypocotyl bending. Lastly, *ARF8* functions in hypocotyl elongation, and it is involved in auxin homeostasis (Tian et al., 2004). The biological functions, however, of the remaining *ARF* gene family members are unknown.

Here, we have employed a functional genomic strategy that involves the identification of T-DNA insertion in the *ARF* gene family members to elucidate some of the biological functions of the ARF transcription factors. Most of the single *arf* T-DNA insertion mutants fail to show an obvious growth phenotype. However, double mutants, such as *arf7 arf19*, show a strong auxin phenotype that results in the absence of lateral root formation than neither the *arf7* nor *arf19* single mutant expresses. The results suggest that there are unique and overlapping functions among related *ARF* gene family members in Arabidopsis.

RESULTS

The Arabidopsis *ARF* Gene Family

The Arabidopsis genome contains 23 *ARF* genes scattered among the five chromosomes (Arabidopsis Genome Initiative, 2000; annotation version V5.0, Figure 1A). The locations of the four previously described loss-of-function mutations, *arf3/ett* (Sessions and Zambryski, 1995), *arf5/mp* (Hardtke and Berleth, 1998), *arf7/nph4* (Harper et al., 2000), and *arf2/hss* (Li et al., 2004), are highlighted in Figure 1A. A cluster of *ARF* genes, *ARF12*, *13*, *14*, *15*, *20*, *21*, and *22*, is present in the upper arm of chromosome I (Figure 1A). These genes share a high degree of similarity among their amino acid and nucleotide sequences (see Supplemental Figure 1 and Table 1 online). *ARF23* is a pseudogene (see Supplemental Figure 1 online; Guilfoyle and Hagen, 2001). Phylogenetic analysis reveals that the genes fall into three branches (marked with different colors in Figure 1B). Class I has the most members (15) that can be subdivided into three subclasses, Ia (five members, shaded brown), Ib (eight members, shaded blue), and Ic (two members, shaded green). Their middle region is rich in Pro, Ser, Gly, or Leu (Guilfoyle and Hagen, 2001; see Supplemental Figure 1 online), and some of them function as repressors (Ulmasov et al., 1999b; Tiwari et al., 2003). Class II (shaded pink) has five members, and some of them function as activators. Their middle region is rich in Glu (Ulmasov et al., 1999a; Guilfoyle and Hagen, 2001). Class III (shaded yellow) also contains three members that are the most divergent compared with those encoded by the other two classes. *ARF3* and *ARF17*, which are considered to lack the C-terminal domains III and IV (Guilfoyle and Hagen, 2001), may potentially contain highly divergent domains III and IV (see Supplemental Figure 1 online). Furthermore, *ARF13* does not have domains III and IV in this new alignment (see Supplemental Figure 1 online). The ARF polypeptides vary in size ranging from ~57 (*ARF13*) to ~129 kD (*ARF7*) (see Supplemental Table 2 online). This size variation is primarily attributable to the different amino acid content in the middle region (see Supplemental Figure 1 online).

RNA hybridization analysis reveals that *ARF1-ARF9*, *ARF11*, *ARF16*, *ARF17*, *ARF18*, and *ARF19* are expressed in light-grown seedlings and various plant tissues, including roots, leaves, flowers, and stems (Ulmasov et al., 1999a; data not shown). We were unable to detect expression of the clustered *ARF* genes in these various RNAs, and there are no ESTs or cDNAs for these genes in public databases. Exploratory RT-PCR analysis using cDNA from various tissues (see Methods) revealed that the clustered genes are expressed during embryogenesis (see Supplemental Figure 2B online). Transgenic plants expressing the β-glucuronidase (*GUS*) reporter gene from the *ARF12* and *ARF22* promoters show that the Pro_{ARF12}:*GUS* is expressed only in the developing seeds, and its expression is detected in the entire seed, including embryos and the integument surrounding the embryo (see Supplemental Figure 2F online). Pro_{ARF22}:*GUS* transgenic plants display an identical GUS expression pattern as the Pro_{ARF12}:*GUS* plants (data not shown).

Isolation of *ARF* T-DNA Insertion Mutants

We initiated this project using a PCR-based screening approach to identify T-DNA insertion mutants for a large number of *ARF* genes. A total of 80,000 T-DNA insertion line populations in the Columbia ecotype were initially screened, and eight lines were identified (Alonso et al., 2003). Subsequently, the laboratory participated in generating the garlic lines in collaboration with the former Torrey Mesa Research Institute, and 10 additional lines

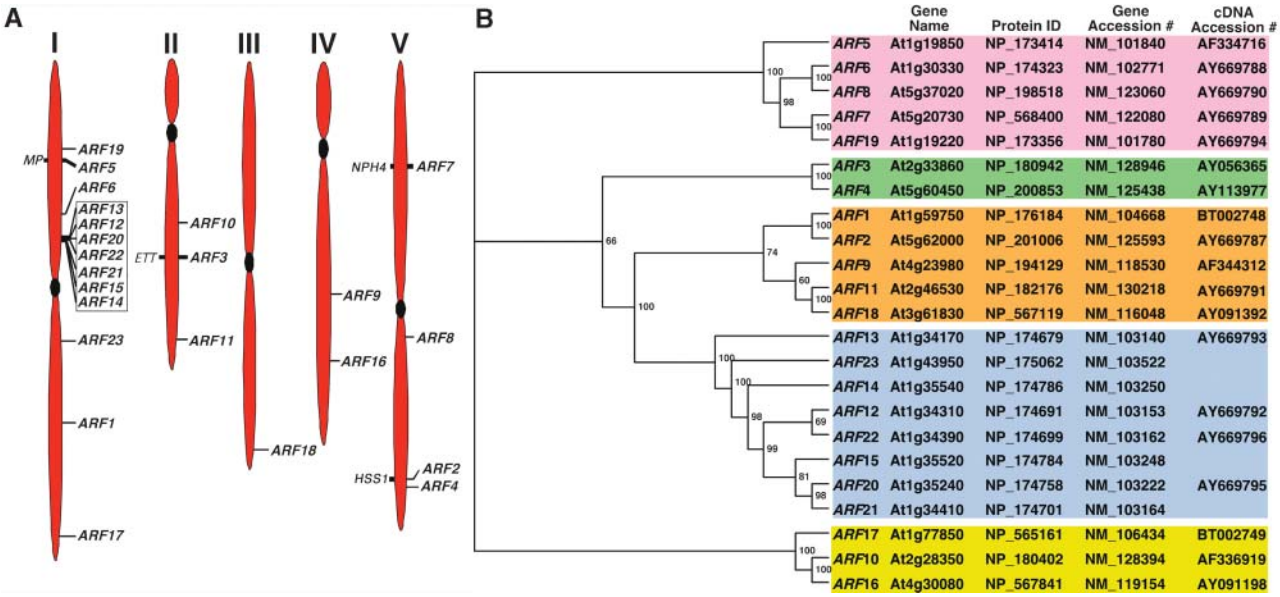

Figure 1. The *ARF* Gene Family of Arabidopsis.

(A) Chromosomal location of *ARF* genes. The locations of 23 putative *ARF* genes on the Arabidopsis chromosomes (I to V) are shown according to version 5.0 of the Arabidopsis Genome annotation submitted to GenBank. Mutants that have been isolated in the *ARF* gene are shown on the left side of the chromosomes. The *ARF* genes clustered on chromosome I are boxed.

(B) Phylogenetic analysis. An unrooted dendogram was generated using ClustalW (Thompson et al., 1994). TreeView was used to generate the graphical output (Page, 1996). The numbers at the branching points indicate the percentage of times that each branch topology was found during bootstrap analysis ($n = 1000$). The gene names, accession numbers, protein identifier, and the accession numbers of the full-length open reading frames (ORFs) used for this analysis are also shown. Predicted ORFs from the genomic annotation were used for *ARF14*, *ARF15*, *ARF21*, and *ARF23* (pseudogene) genes. The full-length ORFs of *ARF2*, *ARF6*, *ARF7*, *ARF8*, *ARF11*, *ARF12*, *ARF13*, *ARF19*, *ARF20*, and *ARF22* were constructed during this study. A differential spliced form of *ARF13* has been cloned recently (accession number AY680406).

were isolated (Sessions et al., 2002). More recently, we obtained another nine T-DNA insertional lines from the Salk T-DNA express line collection (http://signal.salk.edu/cgi-bin/tdnaexpress). Taken together during the last 6 years, we identified 27 T-DNA insertion lines located in the coding region of 18 *ARF* genes. Figure 2 and Supplemental Table 3 online provide a summary of all the mutants isolated and characterized during the course of this study. All the lines have been backcrossed at least once and partially characterized phenotypically. We plan to deposit all the lines in the Arabidopsis Biological Resource Center (http://www.biosci.ohio-state.edu/~plantbio/Facilities/abrc/abrchome.htm) for further molecular and phenotypic characterization by the community.

Phenotypes of Insertion Mutants

We were able to identify T-DNA insertion lines for *arf3/ettin*, *arf5/mp*, *arf7/nph4/msg1*, and *arf2/hss*, and their reported phenotypes were confirmed. Two independent *arf3* alleles, *arf3-1* and *arf3-2*, have unusual gynoecium and floral patterning defects, including an increased number of sepals and carpals (see Supplemental Figures 3A to 3C online; Sessions et al., 1997). The *arf5-1* mutant fails to form root meristem and normal cotyledons (see Supplemental Figure 3D online; Hardtke and Berleth, 1998), and the *arf7-1* mutant displays an impaired phototropic response toward blue light (Figure 4F; Harper et al., 2000). The *arf2-6*, *arf2-7*, and *arf2-8* mutants have a pleiotropic phenotype, including a long, thick, and wavy inflorescence stem, large leaves, abnormal flower morphology, and late flowering under long-day conditions (see Supplemental Figure 3E online; Li et al., 2004; Y. Okushima and A. Theologis, unpublished data). It has been recently reported that *arf8* seedlings have long hypocotyls in various light conditions (Tian et al., 2004). We did not examine the light-associated phenotype of *arf8*, but we saw longer inflorescence stems in the mutant than those in the wild type (Figure 3). The rest of the insertion lines did not show any obvious growth phenotype (Figure 3).

Because most of the *arf* T-DNA insertion mutants fail to show an abnormal growth phenotype (Figure 3), we are generating double and higher-order mutants among the various insertion lines. So far, we have generated double mutants among closely related ARF genes, such as *arf1 arf2*, *arf6 arf8*, and *arf7 arf19* (see Supplemental Figure 4 online). The phenotype of *arf1 arf2* is similar but much stronger than that of *arf2* (see Supplemental Figure 4A online; Li et al., 2004). *ar6 arf8* has dwarfed aerial tissue and exhibits severe defects in flower development (see Supplemental Figure 4C online). The phenotypic and molecular characterization of *arf7 arf19* is presented below.

Isolation and Characterization of *arf7 arf19* Double Mutants

ARF7 and *ARF19* are phylogenetically related (Figure 1B; Liscum and Reed, 2002; Remington et al., 2004). Given the close

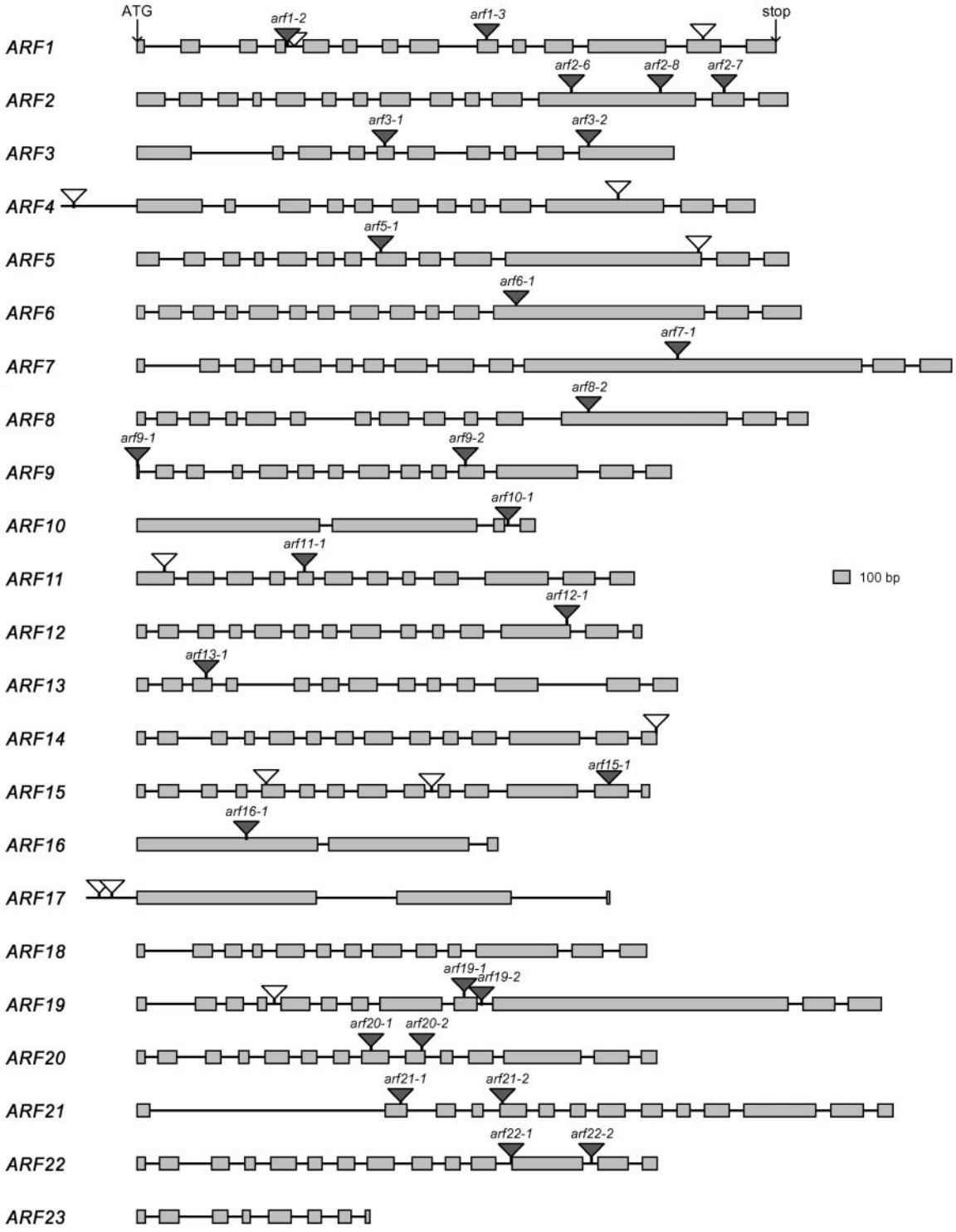

Figure 2. Location of T-DNA Insertions in the *ARF* Gene Family Members.

Boxes represent exons. T-DNA insertions with gray triangles denote lines whose characterization has been completed. T-DNA insertions with white triangles denote lines not yet characterized.

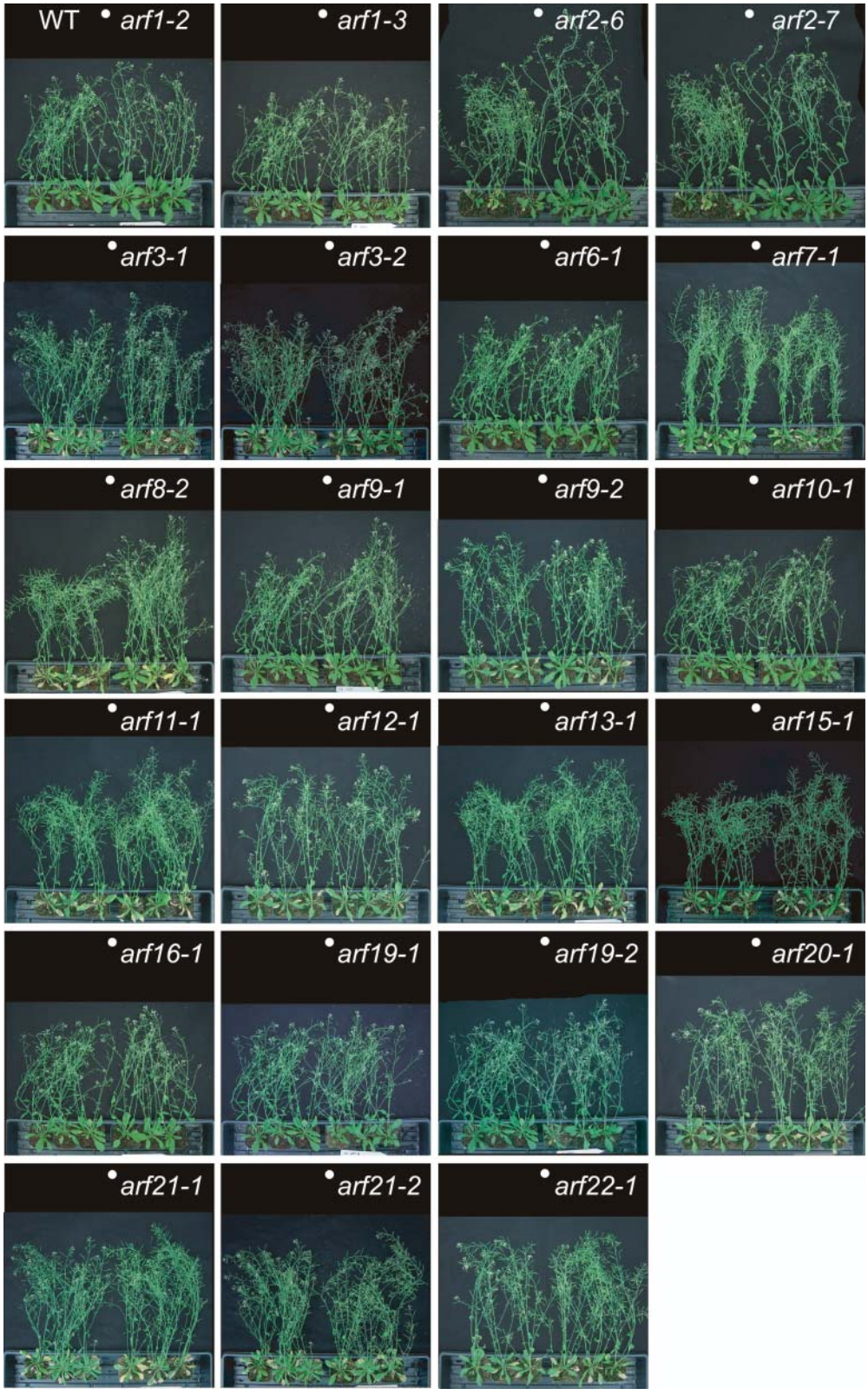

Figure 3. Phenotype of Mature Mutant Plants.

Three wild-type (left) and three mutant plants (right) are shown. The plants were grown at the same time. White dots indicate the boundaries between the wild-type and the mutant plants.

relationship of *ARF7* and *ARF19*, we tested whether the *arf19* mutant had an altered phototropic response similar to that reported for *nph4*/*arf7* (Liscum and Briggs, 1995). We found that the *arf19-1* mutant hypocotyl responded to blue light in a wild type–like manner (Figure 4F). Mature *arf7* mutant plants (*nph4-1*, *arf7-1*, and *msg1-2*/*nph4-102*) do not show any gross developmental defects, except that they have epinastic rosette leaves and the length of the inflorescence stems is slightly shorter than that of the wild-type plants (Figure 3; data not shown; Watahiki and Yamamoto, 1997). These characteristics are more pronounced in the *arf7 arf19* double mutant. The appearance of mature *arf19* plants is identical to that of the wild type (Figures 3 and 4A). The results suggest that the expression of *ARF7* functionally compensates for the loss of *ARF19* expression responsible for differential hypocotyl growth, but not vice versa.

We initially used the *nph4-1* mutant (Liscum and Briggs, 1995) as the *arf7* allele for crossing into *arf19-1* to generate the *arf7 arf19* double mutant. Among the F2 population, approximately one out of 16 plants had short and thin inflorescence stem and small leaves. PCR analysis confirmed that these small plants were double homozygous for both mutations. Because the original *nph4-1* line was screened from fast neutron-mutagenized seeds carrying the homozygous recessive *glabrous1* (*gl1*) mutation (Liscum and Briggs, 1995), we backcrossed the *nph4-1* and *nph4-1 arf19-1* to Columbia (Col) wild-type plants. The *nph4-1* and *nph4-1 arf19-1* mutant lines without the *gl1* mutation were used for further analysis.

The *nph4-1 arf19-1* double mutant exhibits much stronger auxin-related phenotypes than those of *nph4-1* and *arf19-1* single mutants. Adult *nph4-1 arf19-1* mutant plants have thin and short inflorescence stems, and their rosette leaves are small and epinastic (Figures 4A to 4C; see Supplemental Figure 4 online; data not shown). In addition, *nph4-1 arf19-1* has reduced numbers of inflorescence stems, suggesting enhanced apical dominance. By contrast, the flowers of *nph4-1 arf19-1* appear to be normal, and they fertilize normally (data not shown). The phenotype of *nph4-1 arf19-1* is the most obvious at its seedling stage, with its most prominent phenotype being severely impaired lateral root formation (Figure 4B, Table 1). The primary roots of *arf19-1* produce as many lateral roots as the wild type, whereas the *arf7* mutant produces fewer lateral roots compared with the wild type (Figure 4B, Table 1). The primary roots of the *nph4-1 arf19-1* seedlings fail to produce lateral roots in 2-week-old seedlings. However, *nph4-1 arf19-1* seedlings start to generate several lateral roots after ~2 weeks of growth, and their morphological appearance is normal (Figure 4C; data not shown). The *nph4-1 arf19-1* mutant also displays agravitropic responses in both hypocotyls and roots (Figure 4D). When seedlings are grown vertically under dark conditions, the hypocotyl growth orientation of *arf7* is significantly skewed compared with the wild type, whereas the *arf19-1* mutant has a normal gravitropic response (Figure 4D; Harper et al., 2000). Interestingly, in the *nph4-1 arf19-1* seedlings, regulation of growth orientation is disrupted in both hypocotyls and roots, with the hypocotyls occasionally growing downward and the roots upward (Figure 4D). Also, the roots and hypocotyls of *nph4-1 arf19-1* show reduced gravitropic curvatures compared with the wild type when vertically dark-grown seedlings are reoriented by 90° (data not shown). The phototropic response toward blue light in hypocotyls of *nph4-1 arf19-1* seedlings is disrupted as in the *arf7* single mutants (Figure 4F). We generated additional combinations of *arf7 arf19* double mutants using other alleles of *arf7* and *arf19* to confirm the phenotypes of *nph4-1 arf19-1*. We used *msg1-2*/*nph4-102* (Watahiki and Yamamoto, 1997) and *arf7-1* as the *arf7* alleles for crosses with *arf19-1* and *arf19-2*. All five additional *arf7 arf19* double mutant alleles, *msg1-2 arf19-1*, *arf7-1 arf19-1*, *nph4-1 arf19-2*, *msg1-2 arf19-2*, and *arf7-1 arf19-2* (Figures 4A, 4B, and 4D, Table 1; data not shown), display the same phenotypes as *nph4-1 arf19-1*: smaller plant size, impaired lateral root formation, and agravitropic response. These results confirm that the phenotypes of *nph4-1 arf19-1* are caused by the loss of *ARF7* and *ARF19* function.

The phenotypes of the *arf7 arf19* mutant are similar to those reported for the *solitary root* (*slr*)/*iaa14* mutant (Fukaki et al., 2002). The *slr* mutant also shows strong auxin-related phenotypes, including complete lack of lateral roots, agravitropic roots, and hypocotyls, small plant size, and few root hairs (Figures 4A, 4B, and 4D; data not shown). Whereas the *nph4-1 arf19-1* mutant seedlings exhibit severely impaired lateral formation, their primary roots start to produce lateral roots ~2 weeks from germination (Figure 4C). By contrast, *slr-1* seedlings do not produce any lateral roots even after 4 weeks from germination (Figure 4C; data not shown). We also examined the effect of exogenous auxin on lateral root formation in the *nph4-1 arf19-1* seedlings. Four-day-old light-grown seedlings of the wild type, *nph4-1 arf19-1*, and *slr-1* were transferred to medium containing 1 μM IAA. After an additional 3 d of incubation, wild-type seedlings started to produce many lateral roots, but *nph4-1 arf19-1* and *slr-1* fail to produce any lateral roots. However, after 5 d of incubation on IAA, several lateral roots are induced in *nph4-1 arf19-1* but not in *slr-1* (data not shown). Lower concentrations of IAA (1 to 100 nM) fail to induce lateral root formation in *nph4-1 arf19-1* even after 5 d of incubation (data not shown). These results suggest that the auxin- induced lateral root formation is inhibited in *nph4-1 arf19-1*, but is more severely impaired in *slr-1*. Also, both *slr-1* and *arf7 arf19* mutants have smaller size aerial tissues compared with the wild type and single mutants, but *slr-1* has smaller rosette leaves and shorter petioles than *arf7 arf19* (Figure 4C). The most striking phenotypic difference between the *arf7 arf19* and *slr-1* mutants is the root hair formation. The *slr-1* mutant has very few root hairs (Fukaki et al., 2002), whereas the *arf7 arf19* mutant and the *arf7* and *arf19* single mutants show normal root hair formation (Figure 4E).

Auxin Sensitivity of *arf7 arf19*

The *arf7* single mutants display reduced auxin sensitivity in hypocotyl growth, whereas they show normal auxin response in the roots (Figures 5A and 5B; Watahiki and Yamamoto, 1997; Stowe-Evans et al., 1998). By contrast, *arf19-1* shows normal auxin sensitivity in the hypocotyls and a mild but significant resistance to exogenous auxin in the roots (Figures 5A and 5B). The same level of auxin resistance is also observed in the roots of *arf19-2* (data not shown), suggesting that the auxin response is slightly impaired in the roots of the *arf19* single mutants. Interestingly, the *arf7 arf19* double mutants display severely reduced

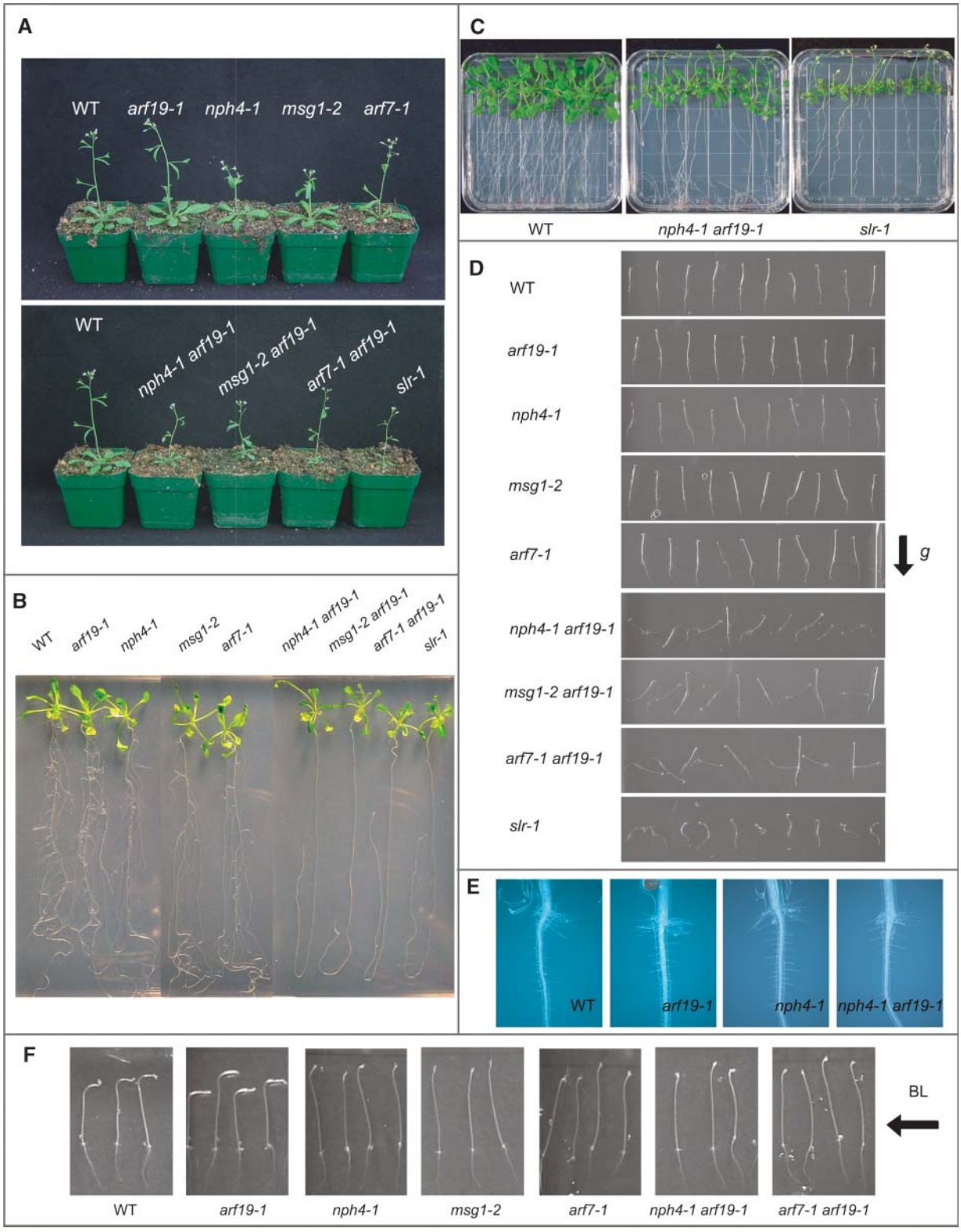

Figure 4. Phenotypes of the *arf7 arf19* Double Mutant.

(A) Four-week-old soil-grown plants of the wild type, *arf19-1*, *nph4-1*, *msg1-2*, and *arf7-1* (top) and the wild type, *nph4-1 arf19-1*, *msg1-2 arf19-1*, *arf7-1 arf19-1*, and *slr-1* (bottom).

Table 1. Lateral Root Formation in *arf7*, *arf19*, and *arf7 arf19* Seedlings

Mutant	Number of Lateral Roots
Wild type (Col)	7.6 ± 3.2
nph4-1	1.3 ± 1.1
msg1-2	0.6 ± 0.7
arf7-1	1.7 ± 1.4
arf19-1	6.8 ± 1.6
nph4-1 arf19-1	0.0 ± 0.0
msg1-2 arf19-1	0.0 ± 0.0
arf7-1 arf19-1	0.0 ± 0.0

The number of lateral roots in 10-d-old seedlings was determined. The numbers represent the average of more than 18 seedlings ± SD.

auxin sensitivity in both roots and hypocotyls (Figures 5A and 5B). The root auxin sensitivity is impaired in *arf7 arf19* to the same degree as in *slr-1.* The data suggest that the hypocotyl auxin sensitivity is impaired in the *arf7* single mutants, the root auxin sensitivity is impaired in the *arf19* single mutants, and both are severely impaired in the *arf7 arf19* double mutant. Surprisingly, the *slr-1* hypocotyls fail to elongate after transfer to dark conditions, and exogenous auxin application does not affect their hypocotyl growth (Figures 5B and 5C).

Expression Patterns of *ARF7* and *ARF19*

We generated transgenic plants with Pro_{ARF7}:*GUS* and Pro_{ARF19}:*GUS* to gain a better understanding of the tissue-specific expression of *ARF7* and *ARF19*. The expression patterns of Pro_{ARF7}:*GUS* and Pro_{ARF19}:*GUS* are distinct, with partial overlap in light-grown seedlings (Figures 6A and 6B). Strong GUS expression is observed in the hypocotyls and petioles of Pro_{ARF7}:*GUS* seedlings (Figure 6A), whereas Pro_{ARF19}:*GUS* expression is restricted to the vascular tissue in the aerial parts (Figure 6B). In root tissue, unlike the aerial part, Pro_{ARF19}:*GUS* is strongly expressed throughout, including vascular tissue, the meristematic region, root cap, root hair, and the sites of newly forming lateral roots (Figures 6B, 6D, and 6J to 6L). By contrast, Pro_{ARF7}:*GUS* expression in the primary root is restricted to the vascular tissues and is not detected in the meristematic region, root cap, and root hairs (Figures 6A, 6C, and 6E to 6I). Pro_{ARF7}:*GUS* is expressed in the early stages of lateral root primordia (Figure 5E). However, after the root primordia emerge from the parental primary roots, the expression of Pro_{ARF7}:*GUS* dissipates from the meristematic region (Figures 6G to 6I). Pro_{ARF7}:*GUS* expression is detected in the vascular tissue after the lateral root is elongated (data not shown). The results suggest that both *ARF7* and *ARF19* are expressed in sites where lateral roots are initiated, consistent with the observation of impaired lateral root formation in the *arf7 arf19* double mutants.

ARF19 Overexpression

Although the loss of *ARF19* function does not alter plant development, overexpression of *ARF19* has a dramatic effect on plant morphology (Figures 7A to 7D). Overexpression of *ARF19* results in alternation of root architecture (Figure 7D). The leaves of Pro_{35S}:*ARF19* plants are narrower, elongated, and misshapen (Figures 7B and 7C). The Pro_{35S}:*ARF19* plants exhibit strong reduction in apical dominance and have a dwarf phenotype (Figure 7A). They produce a small number of siliques and have lower seed production (data not shown). The phenotype of Pro_{35S}:*ARF19* plants is associated with higher levels of the *ARF19* transcript (Figure 7E).

Transcriptional Profiling of the *arf7*, *arf19*, and *arf7 arf19* Mutants

The auxin-related phenotypes of *arf7*, *arf19*, and *arf7 arf19* mutants prompted us to perform detailed microarray analysis with these mutants using the Affymetrix whole-genome ATH1 GeneChip. We used the *nph4-1*, *arf19-1*, and *nph4-1 arf19-1* mutants as representatives for each mutant allele during this experiment. Light-grown seedlings of the wild type, *nph4-1*, *arf19-1*, and *nph4-1 arf19-1* were treated for 2 h with the carrier solvent ethanol (control sample) or 5 μM IAA (auxin-treated sample). Each experiment was performed in triplicate, and total RNA was independently isolated to generate biotin-labeled cRNA for hybridization (see Methods).

Figure 8 shows the scatter plots representing the auxin-regulated transcriptional profiles of wild-type, *arf19-1*, *nph4-1*, and *nph4-1 arf19-1* mutants. A cursory examination of these scatter plots demonstrates that the loss of *ARF7* and *ARF19* causes gross changes in auxin-induced gene expression. The wild-type scatter plot shows that the gene expression profile is globally altered by exogenous auxin treatment. The scatter plot of *arf19-1* shows a similar degree of distribution as with the wild type, suggesting that almost normal auxin-regulated gene expression is maintained in the *arf19* single mutant (Figure 8). However, the scatter plots of *nph4-1* and *nph4-1 arf19-1* display a smaller degree of distribution than that of the wild type, indicating that the auxin-mediated transcriptional regulation is

Figure 4. (continued).

(B) Seventeen-day-old seedlings of wild type, *arf19-1*, *nph4-1*, *msg1-2*, *arf7-1*, *nph4-1 arf19-1*, *msg1-2 arf19-1*, *arf7-1 arf19-1*, and *slr-1*.

(C) Twenty-two-day-old seedlings of the wild type, *nph4-1 arf19-1*, and *slr-1* grown on agar plates vertically.

(D) Gravitropic response of 3-d-old dark-grown seedlings of the wild type, *arf19-1*, *nph4-1*, *msg1-2*, *arf7-1*, *nph4-1 arf19-1*, *msg1-2 arf19-1*, *arf7-1 arf19-1*, and *slr-1*.

(E) Root hair formations of the wild type, *arf19-1*, *nph4-1*, and *nph4-1 arf19-1*.

(F) Phototropism of 3-d-old dark-grown seedlings of the wild type, *arf19-1*, *nph4-1*, *msg1-2*, *arf7-1*, *nph4-1 arf19-1*, and *arf7-1 arf19-1*. Seedlings were exposed to unilateral blue light from the right for 8 h.

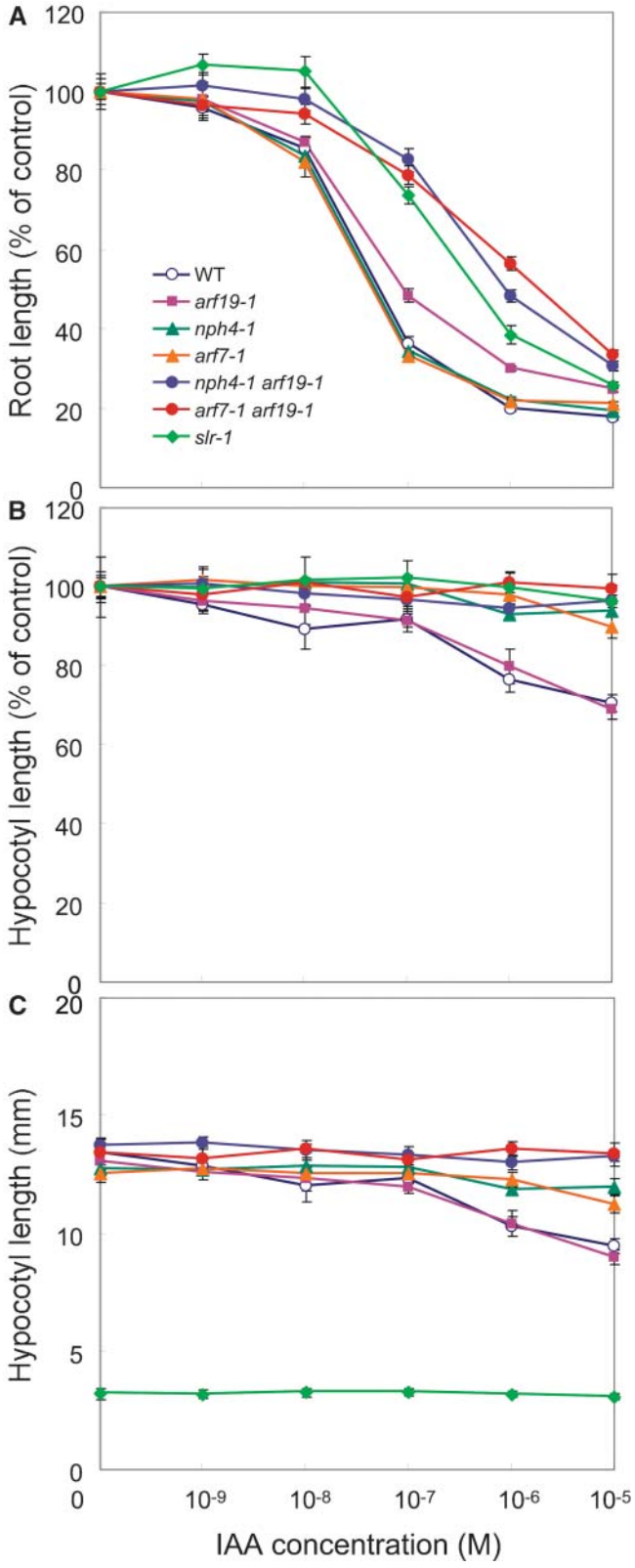

Figure 5. Auxin Sensitivity of the Wild Type, *arf7*, *arf19*, *arf7 arf19*, and *slr* Mutants.

(A) Inhibition of root growth by exogenous auxin. Each value represents the average of more than 10 seedlings. Bars represent SE of the average. **(B)** and **(C)** Inhibition of hypocotyl elongation by exogenous auxin. Data represent the mean of hypocotyl length as a percent of controls **(B)** or of actual measurements **(C)**. Bars represent SE of the average. See Methods for experimental details.

globally repressed in these mutants (Figure 8). We extracted the auxin-regulated genes using the $\log_2$ expression values from the robust multichip analysis (RMA) output file (Irizarry et al., 2003) and established rigorous statistical criteria based on a variance measurement to generate auxin-regulated gene lists (see Methods). Among the 22,800 genes, only 203 met the criteria for more than twofold auxin induction (I, induced genes), and 68 genes met the criteria for more than twofold repression (R, repressed genes). A complete list of all the auxin-regulated genes and how they are affected by the mutants can be found in the Supplemental Tables 4 and 5 online. These gene lists include various classes of known auxin-regulated genes, such as *Aux/IAA*, *GH3*, *SAUR*, and *ACS*, consistent with similar studies reported previously (Tian et al., 2002; Ullah et al., 2003; Redman et al., 2004). The genes identified as auxin-regulated (induced or repressed) were functionally categorized to examine the auxin-regulated cellular and metabolic processes affected by either or both loss-of-function mutations of *ARF7* and *ARF19*. Supplemental Figure 6 online shows their functional classification. Approximately 80% of the auxin-regulated genes is currently annotated as encoding proteins of known or putative function.

We subsequently extracted the gene sets that were induced or repressed by auxin in the wild type, which do not respond, or were only slightly responsive to auxin in the mutants (see Methods). Among the 203 auxin-induced genes, 105 (51.7%), 14 (6.9%), and 173 (85.2%) were identified as differentially regulated genes by *nph4-1*, *arf19-1*, and *nph4-1 arf19-1*, respectively. Likewise, 22 (32.4%), 3 (4.4%), and 44 (64.7%) among the 68 auxin-repressed genes were identified as differentially regulated genes by *nph4-1*, *arf19-1*, and *nph4-1 arf19-1*, respectively. This comparative analysis of differentially regulated genes among the three mutants revealed overlapping genes among these gene sets (Figure 9). For example, among the 203 auxin-induced genes, 96 were similarly affected by the *nph4-1* single and *nph4-1 arf19-1* double mutants (Figure 9A, class I-D). The class I-D genes are considered to be preferentially regulated by *ARF7*. Likewise, eight auxin-induced genes are similarly affected in the *arf19-1* single and *nph4-1 arf19-1* double mutants (Figure 9A, class I-F). These genes are considered to be preferentially regulated by *ARF19*. By contrast, 64 auxin-induced genes are differentially regulated only by the *nph4-1 arf19-1* double mutant (Figure 9A, class I-G). The genes classified into class I-G are considered to be redundantly regulated by both *ARF7* and *ARF19*. Similar distribution of differentially regulated genes is found among auxin-repressed genes (Figure 9B, class R-D to R-G). Supplemental Figure 5 online shows the expression behavior of individual genes that belong to each class (class I-A to I-H and class R-A to R-H). Figure 10 shows the expression behavior of some representative auxin-regulated genes of various functional categories in these

various classes. In addition to classical auxin-regulated genes, such as *IAA5*, *IAA14*, and *IAA19*, various classes of genes involved in ethylene biosynthesis and perception, phytohormone-related, and cell wall biosynthesis and development show defective auxin-regulated gene expression in the mutants,

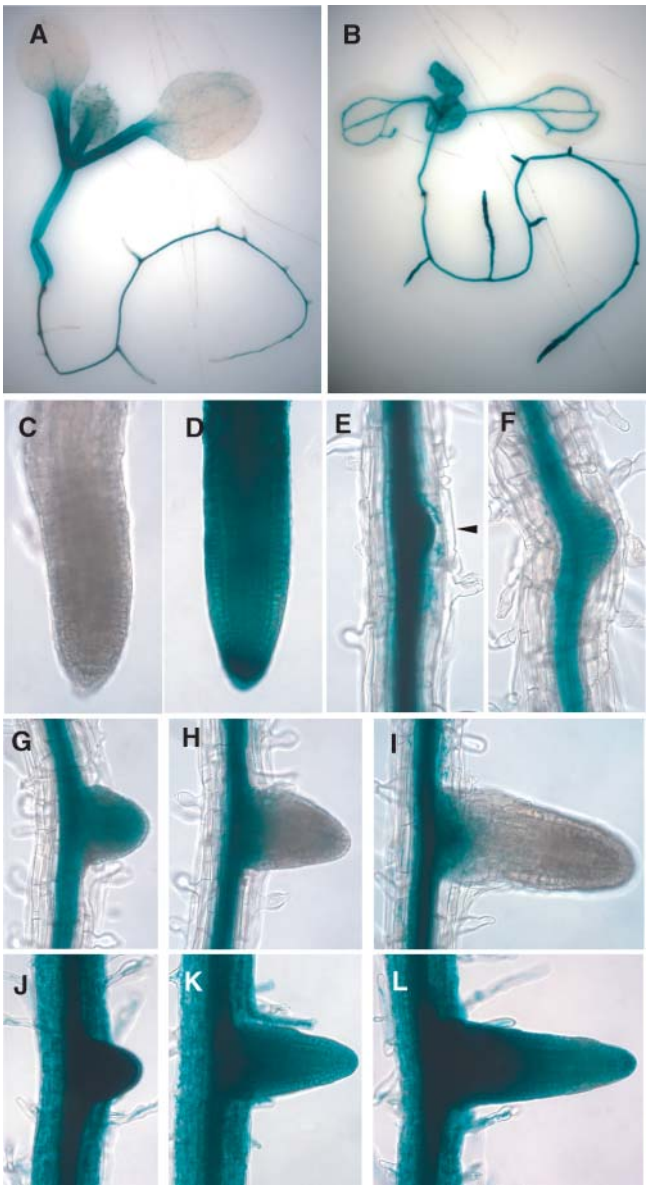

Figure 6. Expression of *GUS* in Pro_{ARF7}:*GUS* and Pro_{ARF19}:*GUS* Transgenics.

(A) GUS expression in a 6-d-old light-grown Pro_{ARF7}:*GUS* seedling.
(B) GUS expression in a 6-d-old light-grown Pro_{ARF19}:*GUS* seedling.
(C) Root apex of a Pro_{ARF7}:*GUS* seedling primary root.
(D) Root apex of a Pro_{ARF19}:*GUS* seedling primary root.
(E) to **(I)** Pro_{ARF7}:*GUS* expression in the vascular tissue of mature primary root, lateral root primordia (**[E]** and **[F]**, arrowhead), and developing lateral roots (**[G]** to **[I]**).
(J) to **(L)** Pro_{ARF19}:*GUS* expression in entire tissue of primary root and developing lateral roots.

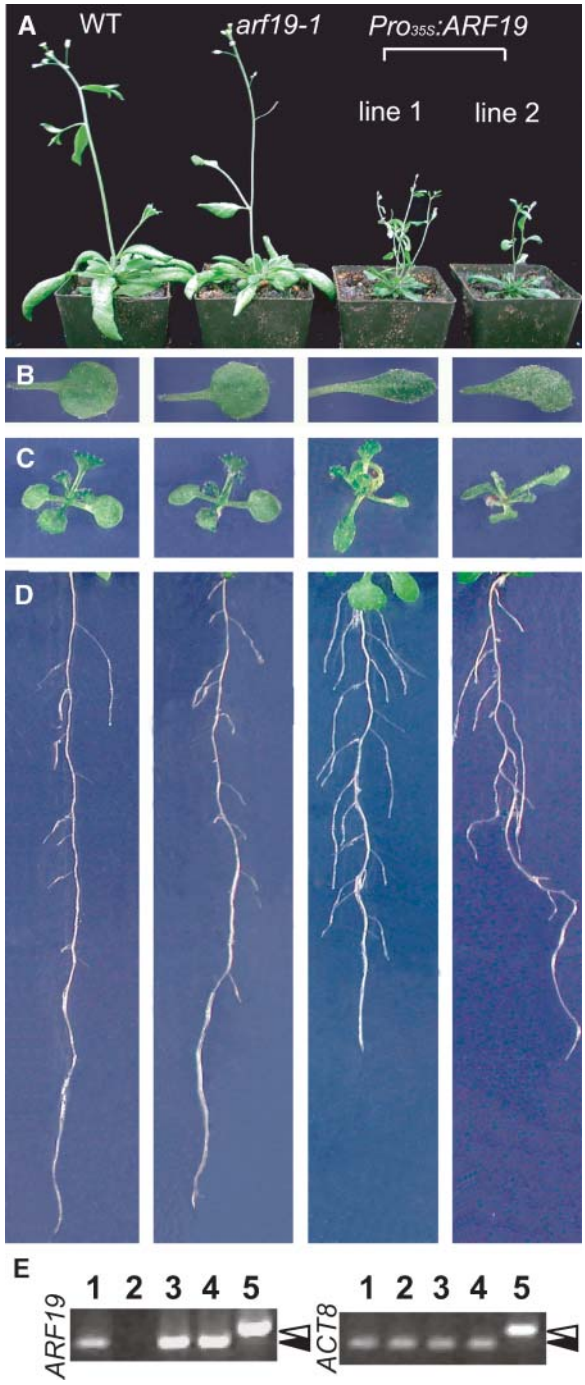

Figure 7. Developmental Defects by *ARF19* Overexpression.

(A) to **(C)** Growth inhibition in 5-week-old plants **(A)**, first true leaves **(B)**, and 12-d-old light-grown seedlings **(C)**.
(D) Alteration of root architecture in 10-d-old seedlings.
(E) Expression of *ARF19* in overexpressing lines from 7-d-old light-grown seedlings. *ARF* gene expression was assessed by RT-PCR as described in Methods. The lanes are as follows: 1, the wild type; 2, *arf19-1*; 3, Pro_{35s}:*ARF19* line 1; 4, Pro_{35s}:*ARF19* line 2; 5, genomic DNA. Accumulation of the *ACT8* transcript was used as an internal control. White and black arrowheads indicate the size of genomic and cDNA fragments, respectively.

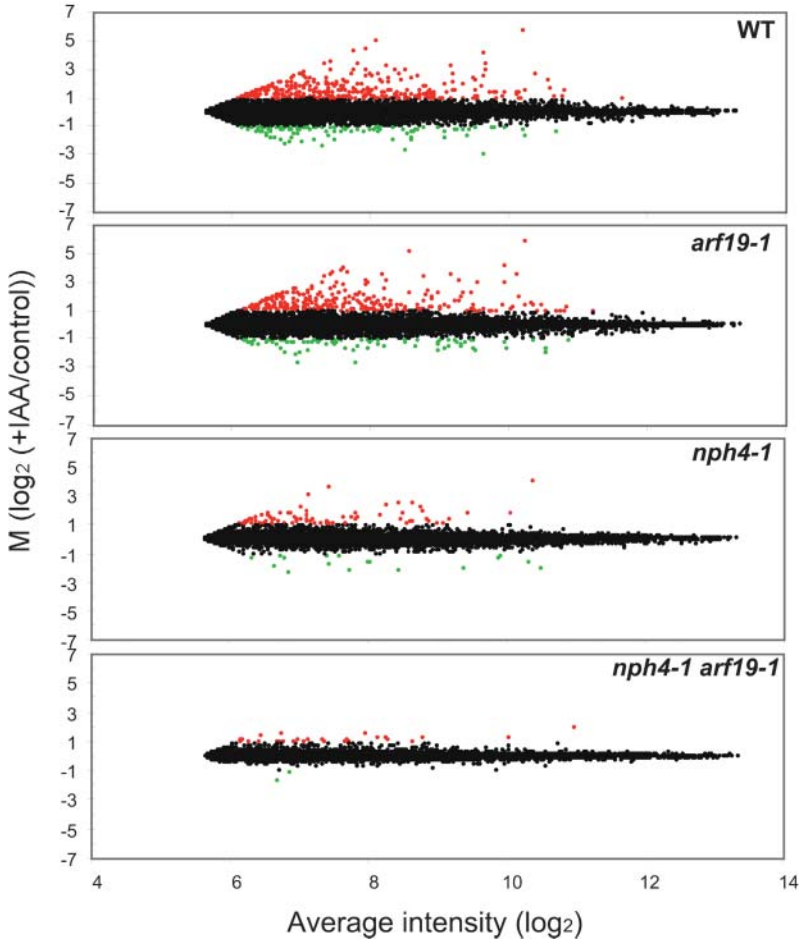

Figure 8. Global Gene Expression Profiling.

MA plots (Dudiot et al., 2002) showing changes of auxin-regulated gene expression levels in the wild type, *arf19-1*, *nph4-1*, and *nph4-1 arf19-1*. Each plot represents the log ratio of the average of the auxin-treated samples (I) to the control samples (C) [$M = \log_2$ (I/C)] versus overall average intensity [$A = \log_2\sqrt{}$(I*C)]. The genes induced by auxin treatment (M > 1) are highlighted in red, and the genes repressed by auxin treatment (M < −1) are highlighted in green. The data were further analyzed for variance to extract statistically valid auxin-regulated genes (see Methods).

especially in *nph4-1 arf19-1*. A wide range of auxin-regulated cellular and metabolic processes is affected by the loss of *ARF7* and *ARF19* gene function.

The transcriptional profile of the untreated control seedlings is also altered in the *nph4-1 arf19-1* double mutant. Comparison of the transcriptional profiles between the *nph4-1 arf19-1* mutant and the wild type in the absence of auxin treatment reveals that 55 and 45 genes are induced and/or repressed twofold or higher in *nph4-1 arf19-1*, respectively (Figure 11; see Supplemental Tables 6 and 7 online). Interestingly, 20 of the 55 induced genes in *nph4-1 arf19-1* are involved in metabolism (see Supplemental Table 6 online). Fewer genes have altered gene expression in untreated *nph4-1* and *arf19-1* seedlings (Figures 11A and 11B). Only two genes are repressed in *arf19-1*, and one of them is *ARF19* itself, suggesting that the *arf19-1* mutation does not affect gene expression in untreated seedlings. Figures 11C and 11D show some representatives of induced or repressed genes in *nph4-1 arf19-1* or both *nph4-1* and *nph4-1 arf19-1*.

DISCUSSION

The *ARF* gene family encodes transcriptional regulators that are involved in auxin signaling. Despite their essential role in auxin-mediated gene regulation, little is known regarding their biological functions, except for very few of them studied by classical molecular genetic analysis. Questions arise, such as why does Arabidopsis have so many ARFs? What is the biological function of each ARF? Which genes do they regulate? To answer these questions, we have attempted to isolate loss-of-function T-DNA insertion mutants for all the *ARF* gene family members using a reverse-genetics strategy. PCR-based reverse genetic screens provide a systematic strategy for analyzing gene function (Borevitz and Ecker, 2004). We have identified T-DNA insertion alleles for 19 out of 23 *ARF* genes, and initial characterization has been conducted for 18 *ARF* T-DNA insertion alleles among the 27 lines isolated. Among the 18 *arf* single mutants, obvious growth phenotypes were observed only in the previously identified

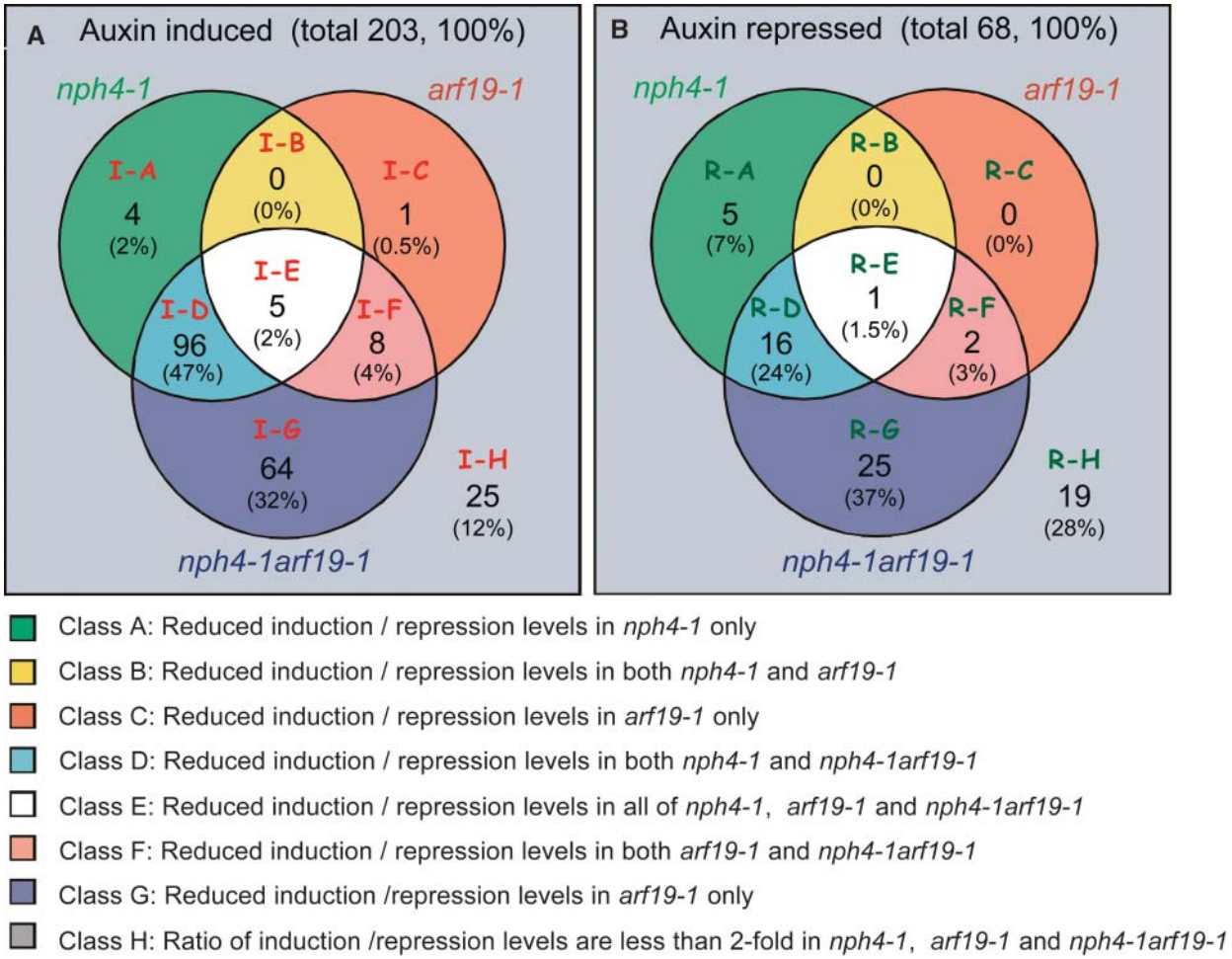

Figure 9. Comparative Analysis of Genes Differentially Regulated by Auxin in *nph4-1*, *arf19-1*, and *nph4-1 arf19-1*.

Differentially regulated genes in mutants among auxin-induced **(A)** and repressed **(B)** genes are shown. Each circle within the Venn diagram indicates numbers and percentages (in parentheses) of genes with repressed induction or repression levels. Only those genes with greater than twofold fold change ratio (FCR) in *nph4-1*, *arf19-1*, and *nph4-1 arf19-1* were analyzed (see Methods). We defined each area of the Venn diagram from A to H, and each class was further divided into two subgroups based on their auxin-induced expression profiles in the wild type. The genes classified into class D are considered to be preferentially regulated by *ARF7*, and those classified into class F are considered to be preferentially regulated by *ARF19*. The genes classified into classes E and G are considered to be redundantly regulated by *ARF7* and *ARF19*. The class A genes have similar expression profiles to class D genes. Likewise, class C genes have similar expression profiles to class F genes. The expression profiles of the representative genes from each class are shown in Supplemental Figure 5 online.

mutants using forward genetics (i.e., *arf2*/*hss*, *arf3*/*ett*, *arf5*/*mp*, and *arf7*/*nph4*). The rest of the *arf* single mutants fail to show an obvious growth phenotype. However, in-depth analysis of these lines regarding their auxin resistance, gravitotropic behavior, and inhibition of root elongation may detect biological phenotypes associated with these lines. These ARFs may act redundantly in auxin-mediated gene regulation and provide compensatory functions during plant development. The expression of at least two clustered *ARF* genes in a specific stage of embryogenesis reinforces the concept of functional redundancy among the ARF proteins. To query the concept of gene redundancy, we generated several double mutants among closely related ARF members. Their phenotypic analysis indicates that related pairs of ARFs, namely, ARF1/ARF2, ARF6/ARF8, and ARF7/ARF19, act redundantly in a distinct developmental manner. During this study, we focused on the redundant functions of *ARF7* and *ARF19* using biological and molecular approaches. A similar picture was recently presented with the *ARF5*/*ARF7* pair (Hardtke et al., 2004). The in planta interaction between ARF5 and ARF7 suggested by the experiments of Hardtke et al. (2004) raises the possibility that different combinations of ARF heterodimers may have various selective functions in regulating targeted gene expression. Potential heterodimerization between ARF7 and ARF19 is also suggested by the inhibition of auxin-induced expession of genes such as At2g23060 (Hookless1-like) and At4g22620 (AtSAUR-34) by either the *arf7* or the *arf19* mutant (see Supplemental Figure 5 online; class I-E). Consequently, the generation of double and higher-order mutants using available *arf*

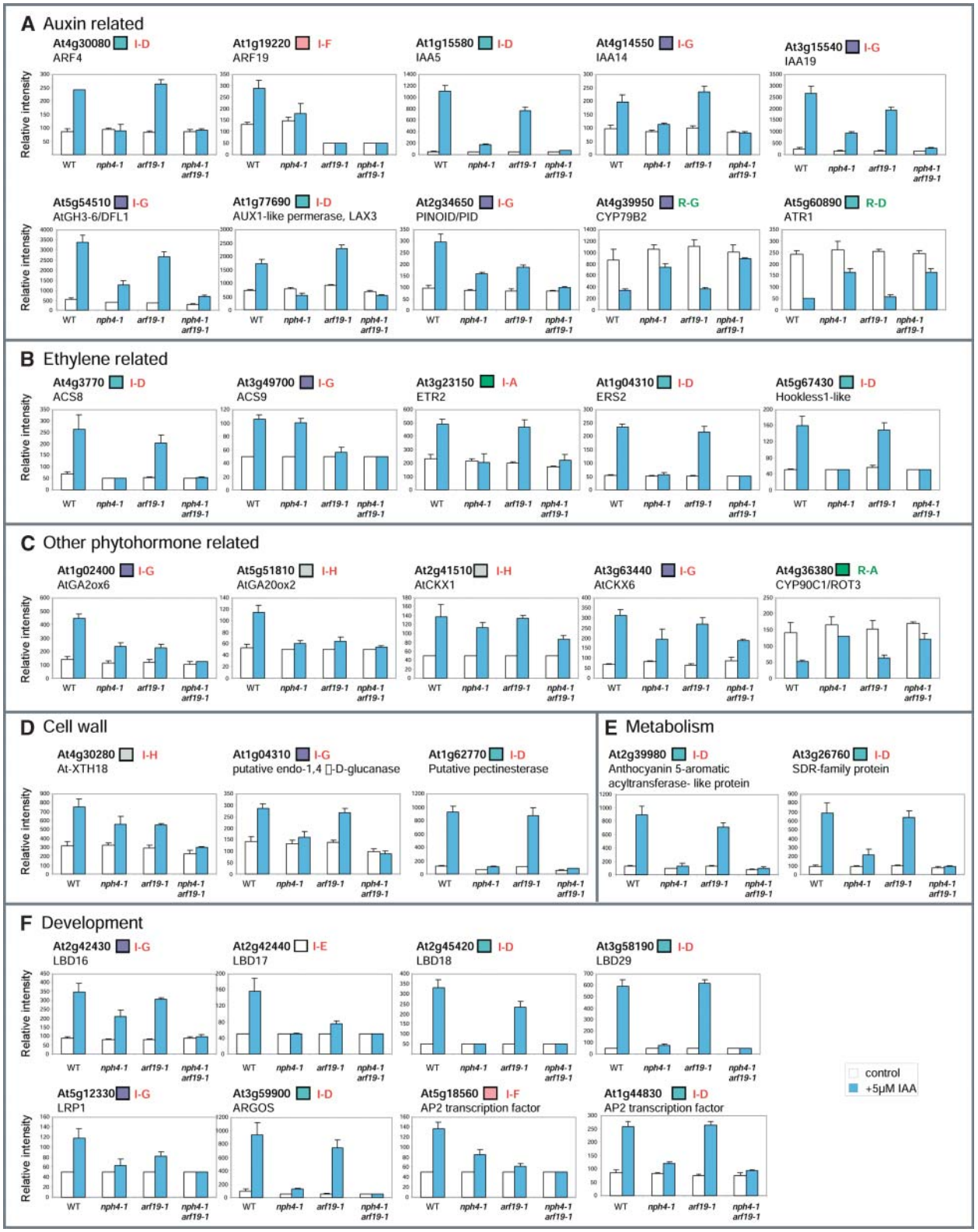

Figure 10. The Expression Profiles of Representative Auxin-Regulated Genes in the Wild Type, *nph4-1*, *arf19-1*, and *nph4-1 arf19-1*.

The data represent the average relative intensity expression level of control (open bar) or auxin-treated (blue bar) samples from triplicate experiments. Bars represent SD of the average. Boxes next to gene names indicate classification color codes according to Figure 9.

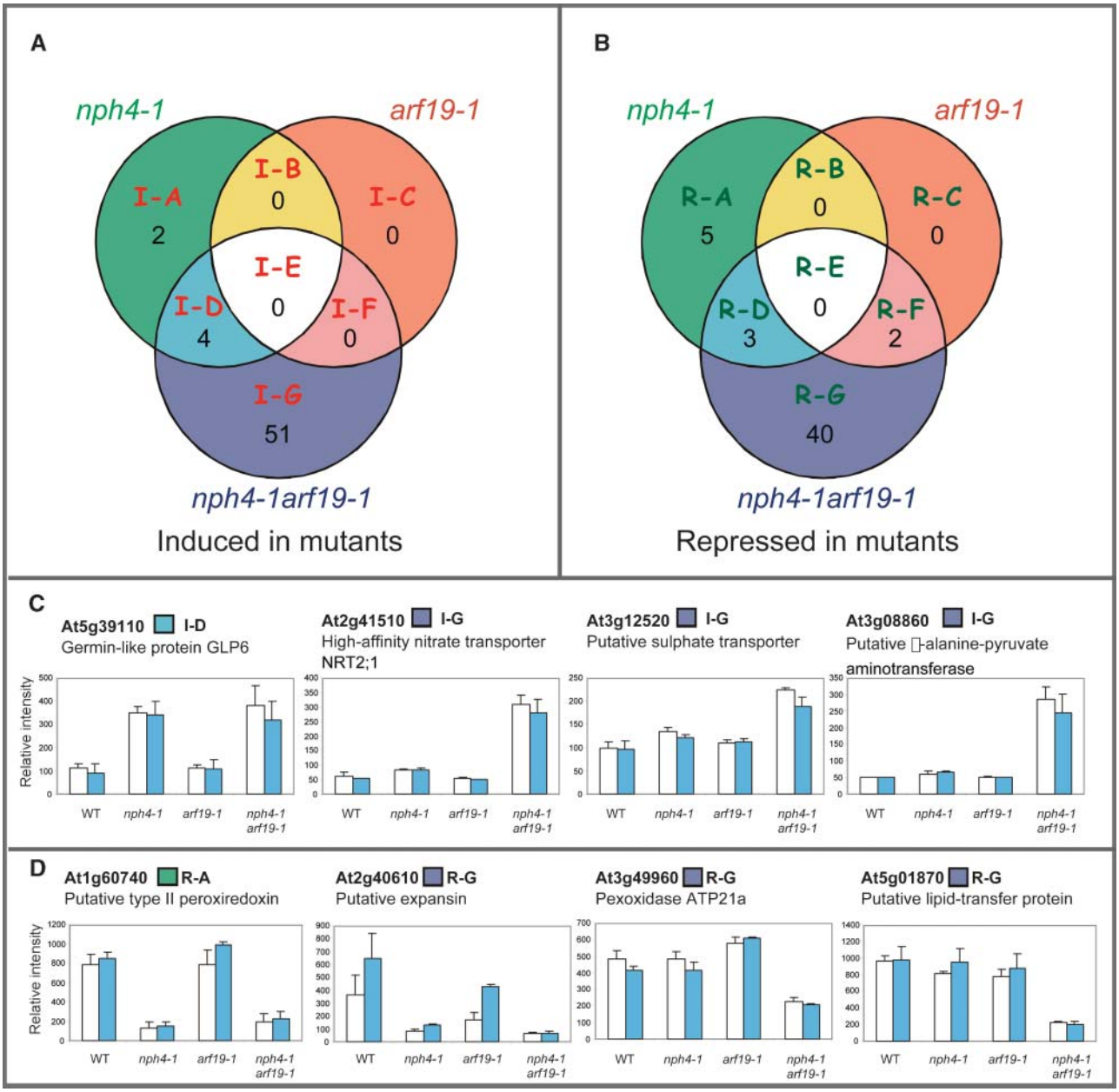

Figure 11. Effect of the *nph4-1*, *arf19-1*, and *nph4-1 arf19-1* Mutations on Global Gene Expression in Untreated Control Samples.

(A) Induced genes in the mutants under control conditions.
(B) Repressed genes in the mutants under control conditions. Each circle within the Venn diagram indicates the number of genes with greater than twofold induction or repression.
(C) Expression profiles of induced classes of genes.
(D) Expression profiles of repressed classes of genes. Data represent the average relative intensity expression levels of control (open bar) or auxin-treated (blue bar) samples from triplicate experiments. Bars represent SD of the average. Boxes next to gene names indicate classification color codes according to **(A)** and **(B)**.

T-DNA insertion mutants will be beneficial to understand auxin-regulated processes mediated by ARF–ARF and ARF–Aux/IAA interactions. Similar studies using reverse genetics have also revealed unique and overlapping functions among the R2R3-MYB and MADS box transcription factor gene family members (Meissner et al., 1999; Parenicova et al., 2003; Pinyopich et al., 2003).

Unique and Overlapping Developmental Functions of *ARF7* and *ARF19*

Considering the phenotypes of *arf7* and *arf19* single mutants, *ARF7* appears to regulate auxin-dependent differential growth in the hypocotyls, and *ARF19* partially mediates auxin signaling in

the roots. The severity of their phenotypes is greatly enhanced in the double mutant compared with the single mutations, demonstrating redundant functions between *ARF7* and *ARF19*. The *arf7 arf19* mutant exhibits strong auxin-related phenotypes, including severely impaired lateral root formation, agravitropic hypocotyls and roots, and small organs and enhanced apical dominance in aerial portions. These phenotypes are observed only in the *arf7 arf19* double mutant, but not in the single mutants, indicating that these developmental events are redundantly regulated by *ARF7* and *ARF19*. Expression of one ARF allows for functional compensation for the loss of the other in *arf7* and *arf19* single mutants. This may be because of the high similarity of these two proteins. The analysis of promoter-GUS transgenic plants demonstrated that there is a significant agreement between the expression patterns and the developmental defects in the single and double mutants. Pro_{ARF7}:*GUS* is strongly expressed in the hypocotyls, whereas Pro_{ARF19}:*GUS* is strongly expressed in the roots. Furthermore, expression of Pro_{ARF7}:*GUS* is detected throughout the hypocotyl, whereas the expression of Pro_{ARF19}:*GUS* is restricted to the vascular tissue of the hypocotyls (Figures 6A and 6B). However, despite the global Pro_{ARF19}:*GUS* expression and an altered auxin sensitivity in *arf19* root, only the *arf7* mutants have slightly reduced numbers of lateral roots (Table 1), suggesting that the *ARF7* has a regulatory function in lateral root initiation. The microarray experiments show that the auxin-dependent induction of *ARF19* is impaired in the *nph4-1* mutant (Figure 10A). Interestingly, the promoter region of *ARF19* contains two *AuxREs* (data not shown), suggesting that *ARF7* may directly modulate the expression of *ARF19*. This may provide an alternative explanation for the apparent phenotype of the *arf7* mutants. The inadequate auxin-mediated induction of *ARF19* expression may have an additive effect on the loss of *ARF7* function, yielding an obvious phenotype. We have not tested yet whether the ARF7 and ARF19 proteins can complement the loss of each other. Promoter-swapping experiments using transgenic *arf7* and *arf19* single or double mutants harboring *ARF7* promoter:*ARF19* and *ARF19* promoter:*ARF7* gene constructs have the potential to clarify this issue.

ARF7 and *ARF19* Regulate Both Unique and Partially Overlapping Sets of Target Genes

The microarray data provide clear evidence for the unique and redundant functions of *ARF7* and *ARF19* on auxin-mediated gene expression. The almost complete lack of auxin-mediated transcriptional regulation in the *arf7 arf19* mutant is puzzling (Figure 9). It implies that ARF7 and ARF19 are the only ARF factors that are necessary and sufficient for auxin signaling in 7-d-old light-grown seedlings. Are the rest of the ARFs dispensable? The possibility exists that the majority of auxin-regulated gene expression during this stage of development is mediated by the *ARF7*/*ARF19* pair. It should be noted that the adult *arf7 arf19* plants, although smaller in size, have a normal appearance with normal flowers and fertility, suggesting that the ARF7/ARF19 pair may not be critical for auxin-mediated transcriptional regulation during the development of aerial organs. Such a proposition is supported by the phenotypes of two other ARF mutants, *arf5*/*mp* and *arf3*/*ett*; they control auxin-mediated gene regulation responsible for axial cell and gynoecium patterning during organogenesis, respectively, indicating that *ARF5* and *ARF3* may also act in a particular developmental window. In addition, several single and double *arf* mutants, including *arf2*, *arf1 arf2*, *arf3*, and *arf6 arf8*, have flowers with abnormal morphology and/or poor fertility, suggesting that these *ARFs* may act redundantly in auxin-mediated gene regulation responsible for flower development. Comparative microarray analysis with different double mutants at different developmental stages has the potential to clarify this view. Alternatively, the remaining *ARFs* may regulate genes that are not auxin regulated at that particular developmental stage. The current prevailing view that all ARFs regulate auxin-mediated gene expression has not been tested experimentally with vigor. Finally, the remaining ARFs may regulate genes in a cell-specific manner (distinct cell types) that the microarray analysis fails to detect. This last possibility points to the necessity of conducting global expression studies in specific cell types (Birnbaum et al., 2003).

Comparative analysis of the gene sets in which auxin-mediated regulation was suppressed in *nph4-1*, *arf19-1*, and *nph4-1 arf19-1* mutants allowed us to classify the auxin-regulated genes into gene sets preferentially regulated by ARF7 and ARF19 alone or redundantly regulated by both ARF7 and ARF19 (Figure 9). The data suggest that the *ARF7* and *ARF19* regulate both distinct and partially overlapping sets of target genes (Figure 9). *ARF7* appears to regulate many more auxin-induced genes (47%) than *ARF19* (4%), and ~30% of the auxin-induced genes are redundantly regulated by *ARF7* and *ARF19*. It is of a great interest that 90% of the auxin-induced or -repressed genes contain at least one *AuxRE* (TGTCnC or GnGACA) in their ~2-kb promoter region (data not shown), suggesting that they are directly regulated by these *ARFs*. This suggests that the ARF7 and ARF19 proteins have the capacity to act as transcriptional activators or repressors of various auxin-regulated genes. The current assignment of ARF7 and ARF19 solely as transcriptional activators is not warranted. Although microarray analysis provides useful and a vast amount of information regarding the genes regulated by the *ARF7*/*ARF19* pair, more direct global technologies, such as chromatin immunoprecipitation and DNA CHIP (ChIP:CHIP), have the potential to identify target genes that are regulated by this and other ARF pairs (Ren et al., 2000; Iyer et al., 2001).

The lists of auxin-regulated genes in which expression is inhibited in the mutants contain putative downstream targets of *ARF7* and *ARF19*. *LATERAL ROOT PRIMORDIUM1* (*LRP1*) is one such candidate gene. The expression level of *LRP1* is induced by auxin treatment in the wild type (Figure 10F; Ullah et al., 2003), and its auxin-mediated induction is inhibited in *nph4-1 arf19-1* (Figure 10F). *LRP1* is expressed during the early stage of lateral root primordia (Smith and Fedoroff, 1995), and its inhibition is consistent with impaired lateral root formation in the *nph4-1 arf19-1* mutant. Another potential candidate is the *AUXIN-REGULATED GENE INVOLVED IN ORGAN SIZE* (*ARGOS*) gene, which is inhibited in auxin-treated and -untreated *nph4-1* and *nph4-1 arf19-1* mutants (Figure 10F). Loss-of-function and gain-of-function mutants of *ARGOS* result in smaller and larger plant sizes, respectively (Hu et al., 2003). The small plant size of *arf7 arf19* may be related to the low expression level

of *ARGOS*. Other potential targets of *ARF7* and *ARF19* are the genes encoding *LATERAL ORGAN BOUNDARIES* (*LOB*) domain (*LBD*) family members (Iwakawa et al., 2002; Shuai et al., 2002). The current analysis reveals that four *LBD* genes, *LBD16*, *LBD17*, *LBD18*, and *LBD29*, are induced by auxin, and their auxin-dependent induction is severely impaired in *nph4-1* and *nph4-1 arf19-1* mutants (Figure 10F). All four highly similar auxin-inducible *LBD* genes contain potential *AuxREs* in their regulatory regions (data not shown). Although the function of these *LBD* genes is still unclear, *LOB* is considered to participate in boundary establishment or communication links between the meristems and initiating lateral organs (Shuai et al., 2002). Overexpression of several *LBD* gene family members results in strong morphological changes (Nakazawa et al., 2003). The root-specific expression of *LBD16* and *LBD29* (Shuai et al., 2002) suggests that these two *LBDs* may be involved in lateral root formation. Overexpression of *LBD16* rescues the lateral root phenotype of the *arf7 arf19* double mutant (Y. Okushima and H. Fukaki, unpublished data). Finally, multiple classes of genes encoding auxin conjugating or auxin synthesis enzymes, cell wall–related proteins, metabolic enzymes, and transcription regulators are potential targets of the ARF7/ARF19 pair (Figure 10; see Supplemental Tables 4 and 5 online).

Regulation of ARF7 and ARF19 by IAA14 and Other Aux/IAAs

The phenotypes of the *arf7 arf1*9 mutants are quite similar to those observed in the *iaa14/slr* mutant. Enhanced IAA14 protein level and the loss of both *ARF7* and *ARF19* functions have similar effects, indicating that all three proteins act on the same developmental pathway. Promoter-GUS expression analysis has revealed that the *ARF7*, *ARF19*, and *IAA14* have overlapping expression patterns at least in the root tissue (Fukaki et al., 2002). This raises the prospect that IAA14 may be a molecular partner of ARF7 and ARF19 by forming heterodimers in planta, thereby repressing the activity of these two ARFs. This interaction may inhibit ARF7- and ARF19-mediated transcriptional activation/repression. Division of pericycle cells is blocked during lateral root initiation in the *iaa14/slr-1* mutant (Fukaki et al., 2002). The stronger phenotype of *iaa14/slr* compared with that observed in *arf7 arf19* (i.e., complete lack of lateral roots and few root hairs) may be attributable to the inhibition of other ARFs by the stabilized IAA14 protein. In addition to the *iaa14/slr* mutant, *iaa3/shy2* (Tian and Reed, 1999), *iaa19/msg2* (Tatematsu et al., 2004), and *iaa28-1* (Rogg et al., 2001) also have reduced numbers of lateral roots, whereas the *iaa14* T-DNA insertion mutant (loss of function) has a normal root phenotype (Y. Okushima and A. Theologis, unpublished data). These data suggest that the function of ARF7 and ARF19 may be negatively regulated by multiple Aux/IAA proteins. Similar functional interactions have been proposed between ARF5 and IAA12 (Hamann et al., 2002; Vogler and Kuhlemeier, 2003), IAA19/MSG2 and ARF7 (Tatematsu et al., 2004), and ARF7 and IAA12 (Hardtke et al., 2004). In planta heterodimerization studies using bimolecular fluorescence complementation have the potential to elucidate the heterodimeric interactions among the *Aux/IAA* and *ARF* gene family products (Hu et al., 2002; Tsuchisaka and Theologis, 2004).

METHODS

Materials

The *pBI101* vector was purchased from Clontech (Palo Alto, CA). All chemicals used for this study were American Chemical Society reagent grade or molecular biology grade. Oligonucleotides were purchased from Operon Technologies (Alameda, CA) or synthesized in house with a Polyplex oligonucleotide synthesizer (GeneMachines, San Carlos, CA).

Molecular Biology

Standard protocols were followed for DNA manipulations described by Sambrook et al. (1989). Standard protocols for DNA sequencing were used to confirm the accuracy of the DNA constructs.

Plant Growth Conditions

Arabidopsis thaliana ecotype Col was used throughout this study. Seeds were surface sterilized for 8 min in 5% sodium hypochlorite + 0.15% Tween-20, excessively rinsed in distilled water and plated on 0.8% agar plates containing 0.5× MS salts (Life Technologies, Rockville, MD) + 0.5 mM Mes, pH 5.7, + 1% sucrose + 1× vitamin B5. The plates were incubated in the dark at 4°C for 2 d and were subsequently transferred to a 16-h-light/8-h-dark cycle at 22°C for light-grown seedlings or in the dark for etiolated seedlings. Mature plants were also grown under the light conditions mentioned above. The root auxin sensitivity assay was performed as follows: 4-d-old light-grown seedlings were transferred to vertically oriented agar plates containing appropriate concentrations of IAA. The root length was determined after an additional 5 d of growth. The auxin sensitivity assay for hypocotyl elongation was performed with 3-d-old seedlings grown on plates lacking auxin and then was transferred to the plates containing various concentrations of IAA and grown for an additional 5 d in the dark. The root and hypocotyl lengths were determined using the NIH Image 1.63 program (http://rsb.info.nih.gov/nih-image/download.html). The phototropic response of etiolated seedlings to blue light was performed as previously described by Liscum and Briggs (1995). Three-day-old etiolated seedlings were exposed to unilateral blue light (1 μmol m^{-2} s^{-1}) for 8 h and then photographed.

Identification and Characterization of T-DNA Insertion Alleles

Screening for T-DNA Insertions

The identification of insertional mutants was performed using a PCR-based screen. For each gene, a forward (F) primer annealing to 100 to 150 bp 5′ of the ATG and a reverse (R) primer annealing to 100 to 150 bp 3′ of the translation stop codon were designed. The size of the genomic products ranged from 6 to 3.2 kb. Eight sets of DNA template derived from 10,000 plants each (80,000 lines total) were screened. Each set of template contained 40 tubes of DNA (10 each of DNA combined from column, row, plate, and individual superpools). Identification of an individual requires a PCR product in each of the four superpools. Using all combinations of F and R primers with primers annealing to the left border and right border of the T-DNA, PCRs were run ($4 \times 40 \times 8 = 1280$ reactions per gene). All operations were adapted to a 384-well format and handling of samples performed with a BioMek robot (Beckman, Palo Alto, CA). The products were analyzed by DNA gel blotting to allow increased sensitivity of detection and assess the specificity of screening. Subsequent to this screen, two large databases containing sequence of DNA flanking T-DNA inserts in 100,000 and 20,000 independent lines have been screened in silico. Data for the 100,000 lines were generated in a collaboration of the University of California, Berkeley, with the Torrey

Mesa Research Institute, and the 20,000 lines have been obtained by SIGNAL (http://signal.salk.edu/cgi-bin/tdnaexpress).

Confirmation of T-DNA Lines

The nature and location of the T-DNA insertion is confirmed by sequencing PCR products. Once the location of the T-DNA insertion was confirmed, we designed gene-specific PCR primers that flank the T-DNA for use in a codominant genotyping analysis. By performing two sets of PCR, one using the gene-specific primer pair and the other using a gene-specific primer and the T-DNA border primer, we could determine whether the individual is homozygous for no T-DNA insertion, heterozygous for the T-DNA insertion, or homozygous for the T-DNA insertion.

Molecular Characterization of the T-DNA Lines

To determine the number of T-DNA inserts present in the lines, we compared the DNA gel blot hybridization patterns arising from sibling plants that were either homozygous for the T-DNA insertion or homozygous for no T-DNA. To remove additional T-DNA loci from the lines of interest, backcrosses to wild-type Col were performed, and plants homozygous for the T-DNA insertion were again identified.

Construction of Promoter-GUS Fusions

The following primers were used to amplify the *ARF* promoter fragments: *ARF7*, F 5′-CTAAGCTTGTCGACAGTACGTAGATTATTTTCCACAACTCTCTC-3′ and R 5′-GAGGATCCATGATCACTCAACTTTACTTTCTCTGAAG-3′; *ARF12*, F 5′-GGAGGTCGACACAAACAACATGATTGAATAAG-3′ and R 5′-GATCGGATCCCCAAAATATGTTATCTCAAC-3′; *ARF19*, F 5′-ACTGAAGCTTTGGGCTAGATTCATCCGTATCTGGGT-3′ and R 5′-CCCGGGAATTCTCATGATGGTTTGGTGCAGGGAAG-3′; *ARF22*, F 5′-GAAGAAGAGTGAAATCCAGTGACC-3′ and R 5′-AGGATCCATAAGCTCGTATCTAAAGCTCGG-3′.

Promoter fragments (*ARF12* and *ARF22*, 2 kb; *ARF7*, 2.5 kb; *ARF19*, 3.2 kb) upstream of the translation initiation codon were synthesized by PCR using wild-type (Col) genomic DNA and the primers listed above. The fragments were sequenced and subcloned into the *pBI101.2* (*ARF7*, *ARF12*, and *ARF22*) or pZP121 (ARF19; Hajdukiewicz et al., 1994) vectors as *Sal*I/*Bam*HI (*ARF7* and *ARF12*), *Hin*dIII/*Bam*HI (*ARF22*), and *Sal*I/*Bsp*HI (ARF19) fragments. The pZP121 vector was modified by introducing the *GUS* gene as an *Nco*I/*Sac*I fragment. Among the four promoter *GUS* constructs, Pro_{ARF12}:*GUS*, Pro_{ARF22}:*GUS*, Pro_{ARF7}:*GUS*, and Pro_{ARF19}:*GUS*, the Pro_{ARF19}:*GUS* promoter also contains 889 bp of the 3′ region of the *ARF19* gene (from the 41-bp 5′ of the *ARF19* translation stop codon to the 848-bp 3′ of the translation stop codon). It was amplified by PCR with the primers, F 5′-ACTGGAGCTCGTACACTATGAAGACACTTCTGCTGCAGCT-3′ and R 5′-TGACGAATTCAAGACGCGATTGAACCAACCCGGTATGA-3′, using BAC T29M8 DNA as a template. It was subcloned as a *Sac*I/*Eco*RI fragment into a *pZP121-*Pro_{ARF19}*-GUS* construct. With the *Sac*I site present in the forward primer and the *Eco*RI site located in the reverse primer, the PCR product was cloned into *pNco*I*-GUS* to create *pGUS-3A11*.

These constructs were introduced into *Agrobacterium tumefaciens* strain GV3101, and wild-type Col plants were transformed by dipping (Clough and Bent, 1998). Kanamycin-resistant plants in the T2 (Pro_{ARF7}:*GUS*) and T3 (Pro_{ARF12}:*GUS*, Pro_{ARF19}:*GUS*, and Pro_{ARF22}:*GUS*) generations were histochemically stained to detect GUS activity by incubating seedlings or tissues in 100 mM sodium phosphate buffer, pH 7.5, containing 1 mM 5-bromo-4-chloro-3-indolyl-β-D-glucuronic acid, 0.5 mM potassium ferricyanide, 0.5 mM potassium ferrocyanide, and 0.1% Triton X-100 for 5 h at 37°C followed by dechlorophylation in 70% ethanol. Several independent lines were examined for GUS staining.

Overexpression of ARF19

Transgenic plants overexpressing the ARF19 protein (Pro_{35S}:*ARF19*) under the control of the *35S* promoter were generated by subcloning the 35S-ARF DNA (pS-A11) as a *Xho*I fragment into the binary vector *pKF111.XL* (Ni et al., 1998) and transforming plants as described (Clough and Bent, 1998). Fifty-two T1 transformants were selected in soil based on resistance to Finale (Farnam Companies, Phoenix, AZ) diluted 1:1,000 (final concentration 0.05% glufosinate ammonium) in 0.005% Silwet, and sprayed on the germinating seedlings. Two lines (line 1 and line 2) were examined in detail.

RT-PCR Analysis

Total RNA was isolated from various stages of flower and silique samples using RNAqueous RNA isolation kit with Plant RNA isolation aid (Ambion, Austin, TX). For each sample, 2.5 μg of total RNA was treated with RQ1 RNase-free DNase (Promega, Madison, WI) to eliminate genomic DNA contamination. First-strand cDNA was synthesized with an oligo$(dT)_{24}$ primer using a SuperScript II reverse transcriptase (Invitrogen, Carlsbad, CA). Then, 1/100th of the resulting cDNA was subjected to 35 cycles of PCR amplification (95°C for 20 s, 62°C for 20 s, 72°C for 45 s). A mixture of *ARF12*, *ARF13*, *ARF14*, *ARF15*, *ARF20*, *ARF21*, and ARF22 cDNA was amplified using primers designed based on the *ARF12* coding region: 5′-TCTGGACACTCCTCCGGTGA-3′ and 5′-TGAGAGACTCTTCCTGGACTTCAAA-3′. Because the nucleotide sequences of *ARF12*, *ARF13*, *ARF14*, *ARF15*, *ARF20*, *ARF21*, and ARF22 cDNA are very similar (see Supplemental Table 1 online), the same expression patterns shown in Supplemental Figure 2B online were also observed when we used primer pairs based on the *ARF21* and *ARF22* coding region (data not shown). The expression level of *ARF19* in wild-type, *arf19-1*, and Pro_{35S}:*ARF19* plants was performed using the primers 5′-ACAAAGGTTCAAAAACGAGGGTCA-3′ and 5′-CGATGGCCCTCGAATGATAATGTAA-3′. *ACT8* gene-specific primers described by An et al. (1996) were used for control amplification.

Microarray Analysis

Surface-sterile seeds (1.8 mg) were germinated in 40 mL of 0.5× MS medium (Life Technologies) containing 1.5% sucrose and cultured in a 16-h-light/8-h-dark cycle with gentle shaking (100 rpm). After a 7-d culture period, the seedlings were treated with 5 μM IAA (IAA treated) or EtOH (control) for 2 h. Total RNA was prepared using RNAqueous RNA isolation kit with Plant RNA isolation aid (Ambion). After LiCl precipitation, RNA was purified using RNeasy columns (Qiagen, Valencia, CA) and reprecipitated with LiCl. RNA pellets were washed with 70% EtOH (three times) and resuspended in diethyl pyrocarbonate–treated water. Five micrograms of total RNA was used for biotin-labeled cRNA probe synthesis. cRNA probe synthesis, hybridization, washing, and scanning and detection of the array image were performed according to the manufacturer's protocols (Affymetrix, Santa Clara, CA). Twenty-four independent hybridization experiments with three independent biological replicates were performed in this study.

Microarray Data Analysis

Affymetrix GeneChip Microarray Suite version 5.0 software was used to obtain signal values for individual genes. The data files containing the probe level intensities (cell files) were used for background correction and normalization using the $\log_2$ scale RMA procedure (Irizarry et al., 2003). The R environment (Ihaka and Gentleman, 1996) was used for running the RMA program. Data analysis and statistical extraction were performed using $\log_2$ converted expression intensity data within Microsoft Excel 98 (Microsoft, Redmond, WA). Based on preliminary analysis, a hybridization signal <5.64 (= $\log_2$ 50) was considered as background; all signals <5.64 were converted to 5.64 before further analysis. The entire data set is

provided in the supplemental data online and has been deposited in the Gene Expression Omnibus database (http://www.ncbi.nlm.nih.gov/geo/) with accession numbers GSE627 and GSM9571 to GSM9594.

We used an *MA*-plot (Dudiot et al., 2002) to represent the difference between two data sets (Figure 10). $M = \log_2 (X/Y)$ and $A = \log_2 \sqrt{X*Y}$ (X and Y are the average expression levels for X and Y data sets, respectively). Also, a *t* value (Dudiot et al., 2002) cutoff was used to identify the statistically valid differentially regulated genes among the two data sets. The *t* value was calculated using the following formulas; $t = M/SE$ ($SE^2 = 1/n^2$ ($var_1 + var_2 \ldots + var_n$); *var* is the variance of the expression intensity of the triplicate experiments; *n* is the number of data sets. A high *t* value corresponds to low variability (high confidence) data, whereas a low *t* value corresponds to high variability (low confidence) data. We use 7 as the cutoff *t* value; data with $|t| < 7$ were excluded from our differentially regulated gene list.

For example, to extract statistically valid auxin-regulated genes in the wild type, (1) we first calculated the ratio of the average gene expression intensities for the auxin-treated samples to control samples (*M*). Genes with $|M| \geq 1$ (twofold or more induced or repressed; $\log_2 2 = 1$) were extracted to generate a preliminary gene list for auxin-regulated genes. At this stage, 294 and 112 genes were identified as auxin induced and repressed genes, respectively. (2) *t* values for auxin-treated and control samples were calculated, and genes with $|t| < 7$ were excluded from the list. After this process, 203 of the 294 auxin induced genes in step (1) met this criterion and were extracted as statistically valid auxin-induced genes. Also, 65 genes among 112 repressed genes in step (1) met this criterion and were extracted as statistically valid auxin-repressed genes. The same procedure was employed to identify the genes with induced or repressed expression levels in mutants. Forty-three, 15, and 145 genes were identified as induced genes in *nph4-1*, *arf19-1*, and *nph4-1 arf19-1* mutants, respectively, in step (1). Among them, 6, 0, and 55 genes passed the step (2) statistical test and then identified as statistically valid induced genes in *nph4-1*, *arf19-1*, and *nph4-1 arf19-1* mutants, respectively. For identification of repressed genes in the mutants, 28, 11, and 100 genes were extracted as repressed genes in *nph4-1*, *arf19-1*, and *nph4-1 arf19-1* by step (1), respectively. Among them, 8, 2, and 45 genes passed the step (2) statistical test and then identified as statistically valid repressed genes in *nph4-1*, *arf19-1*, and *nph4-1 arf19-1* mutants, respectively. To extract the differentially regulated genes in mutants among auxin-regulated genes, we used FCR of induction or repression levels between mutants and the wild type as criteria, with a cutoff FCR value of ≥ 2. Venn diagrams were drawn using GeneSpring software package version 5.1 (Silicon Genetics, Redwood, CA).

Sequence data from this article have been deposited with the EMBL/GenBank data libraries under accession numbers AY669787 to AY669796 and AY680406.

ACKNOWLEDGMENTS

We thank E. Liscum, K. Yamamoto, and H. Fukaki for providing *nph4-1*, *msg1-2*, and *slr-1* seeds, respectively, and T. Speed for helpful discussions regarding microarray data analysis. We also thank D. Hantz for greenhouse work. This research was supported by the National Institutes of Health Grant GM035447 to A.T.

Received October 5, 2004; accepted November 15, 2004.

REFERENCES

Abel, S., Ballas, N., Wong, L.-M., and Theologis, A. (1996). DNA elements responsive to auxin. Bioessays **18,** 647–654.

Abel, S., Nguyen, M.D., and Theologis, A. (1995). The *PS-IAA4/5*-like family of early auxin-inducible mRNAs in *Arabidopsis thaliana*. J. Mol. Biol. **251,** 533–549.

Abel, S., Oeller, P.W., and Theologis, A. (1994). Early auxin-induced genes encode short-lived nuclear proteins. Proc. Natl. Acad. Sci. USA **91,** 326–330.

Abel, S., and Theologis, A. (1996). Early genes and auxin action. Plant Physiol. **111,** 9–17.

Alonso, J.M.A., et al. (2003). Genome-wide insertional mutagenesis of *Arabidopsis thaliana*. Science **301,** 653–657.

An, Y.Q., McDowell, J.M., Huang, S., McKinney, E.C., Chambliss, S., and Meagher, R.B. (1996). Strong, constitutive expression of the *Arabidopsis* ACT2/ACT8 actin subclass in vegetative tissues. Plant J. **10,** 107–121.

Arabidopsis Genome Initiative (2000). Analysis of the genome sequence of the flowering plant *Arabidopsis thaliana*. Nature **408,** 796–815.

Borevitz, J.O., and Ecker, J.R. (2004). Plant genomics: The third wave. Annu. Rev. Genomics Hum. Genet. **5,** 443–477.

Birnbaum, K., Shasha, D.E., Wang, J.Y., Jung, J.W., Lambert, G.M., Galbraith, D.W., and Benfey, P.N. (2003). A gene expression map of the Arabidopsis root. Science **302,** 1956–1960.

Clough, S.J., and Bent, A.F. (1998). Floral dip: A simplified method for *Agrobacterium*-mediated transformation of *Arabidopsis thaliana*. Plant J. **16,** 735–743.

Davies, P.J. (1995). Plant Hormones, Physiology, Biochemistry and Molecular Biology, 2nd ed. (Dordrecht, The Netherlands: Kluwer).

Dharmasiri, N., and Estelle, M. (2004). Auxin signaling and regulated protein degradation. Trends Plant Sci. **9,** 302–308.

Dudiot, S., Yang, Y.H., Callow, M.J., and Speed, T.P. (2002). Statistical methods for identifying differentially expressed genes in replicated cDNA microarray experiments. Statistica Sinica **12,** 111–139.

Fukaki, H., Tameda, S., Masuda, H., and Tasaka, M. (2002). Lateral root formation is blocked by a gain-of-function mutation in the *SOLITARY-ROOT/IAA14* gene of *Arabidopsis*. Plant J. **29,** 153–168.

Gray, W.M., del Pozo, J.C., Walker, L., Hobbie, L., Risseeuw, E., Banks, T., Crosby, W.L., Yang, M., Ma, H., and Estelle, M. (1999). Identification of an SCF ubiquitin-ligase complex required for auxin response in *Arabidopsis thaliana*. Genes Dev. **13,** 1678–1691.

Gray, W.M., Kepinski, S., Rouse, D., Leyser, O., and Estelle, M. (2001). Auxin regulates SCF^{TIR1}-dependent degradation of AUX/IAA proteins. Nature **414,** 271–276.

Guilfoyle, T., Hagen, G., Ulmasov, T., and Murfett, J. (1998). How does auxin turn on genes? Plant Physiol. **118,** 341–347.

Guilfoyle, T.J., and Hagen, G. (2001). Auxin response factors. J. Plant Growth Regul. **20,** 281–291.

Hajdukiewicz, P., Svab, Z., and Maliga, P. (1994). The small, versatile pPZP family of Agrobacterium binary vectors for plant transformation. Plant Mol. Biol. **25,** 989–994.

Hamann, T., Benkova, E., Baurle, I., Kientz, M., and Jurgens, G. (2002). The *Arabidopsis BODENLOS* gene encodes an auxin response protein inhibiting MONOPTEROS-mediated embryo patterning. Genes Dev. **16,** 1610–1615.

Hardtke, C.S., and Berleth, T. (1998). The *Arabidopsis* gene *MONOPTEROS* encodes a transcription factor mediating embryo axis formation and vascular development. EMBO J. **17,** 1405–1411.

Hardtke, C.S., Ckurshumova, W., Vidaurre, D.P., Singh, S.A., Stamatiou, G., Tiwari, S.B., Hagen, G., Guilfoyle, T.J., and Berleth, T. (2004). Overlapping and non-redundant functions of the *Arabidopsis* auxin response factors *MONOPTEROS* and *NONPHOTOTROPIC HYPOCOTYL 4*. Development **131,** 1089–1100.

Harper, R.M., Stowe-Evans, E.L., Luesse, D.R., Muto, H., Tatematsu, K., Watahiki, M.K., Yamamoto, K., and Liscum, E. (2000). The *NPH4* locus encodes the auxin response factor ARF7, a conditional

regulator of differential growth in aerial Arabidopsis tissue. Plant Cell **12,** 757–770.

Hu, C.-D., Chinenov, Y., and Kerppola, T.K. (2002). Visualization of interactions among bZIP and Rel family proteins in living cells using bimolecular fluorescence complementation. Mol. Cell **9,** 789–798.

Hu, Y., Xie, Q., and Chua, N.H. (2003). The Arabidopsis auxin-inducible gene *ARGOS* controls lateral organ size. Plant Cell **15,** 1951–1961.

Ihaka, K., and Gentleman, R. (1996). R: A language for data analysis and graphics. J. Comput. Graph. Statist. **5,** 299–314.

Irizarry, R.A., Bolstad, B.M., Collin, F., Cope, L.M., Hobbs, B., and Speed, T.P. (2003). Summaries of Affymetrix GeneChip probe level data. Nucleic Acids Res. **31,** e15.

Iwakawa, H., Ueno, Y., Semiarti, E., Onouchi, H., Kojima, S., Tsukaya, H., Hasebe, M., Soma, T., Ikezaki, M., Machida, C., and Machida, Y. (2002). The *ASYMMETRIC LEAVES2* gene of *Arabidopsis thaliana*, required for formation of a symmetric flat leaf lamina, encodes a member of a novel family of proteins characterized by cysteine repeats and a leucine zipper. Plant Cell Physiol. **43,** 467–478.

Iyer, V.R., Horak, C.E., Scafe, C.S., Botstein, D., Snyder, M., and Brown, P.O. (2001). Genomic binding sites of the yeast cell-cycle transcription factors SBF and MBF. Nature **409,** 533–538.

Kim, J., Harter, K., and Theologis, A. (1997). Protein-protein interactions among the Aux/IAA proteins. Proc. Natl. Acad. Sci. USA **94,** 11786–11791.

Knauss, S., Rohrmeier, T., and Lehle, L. (2003). The auxin-induced maize gene *ZmSAUR2* encodes a short-lived nuclear protein expressed in elongating tissues. J. Biol. Chem. **278,** 23936–23943.

Li, H., Johnson, P., Stepanova, A., Alonso, J.M., and Ecker, J.R. (2004). Convergence of signaling pathways in the control of differential cell growth in *Arabidopsis*. Dev. Cell **7,** 1–20.

Liscum, E., and Briggs, W.R. (1995). Mutations in the NPH1 locus of Arabidopsis disrupt the perception of phototropic stimuli. Plant Cell **7,** 473–485.

Liscum, E., and Reed, J.W. (2002). Genetics of Aux/IAA and ARF action in plant growth and development. Plant Mol. Biol. **49,** 387–400.

Meissner, R.C., et al. (1999). Function search in a large transcription factor gene family in Arabidopsis: Assessing the potential of reverse genetics to identify insertional mutations in R2R3 *MYB* genes. Plant Cell **11,** 1827–1840.

Nagpal, P., Walker, L.M., Young, J.C., Sonawala, A., Timpte, C., Estelle, M., and Reed, J.W. (2000). *AXR2* encodes a member of the Aux/IAA protein family. Plant Physiol. **123,** 563–573.

Nakazawa, M., Ichikawa, T., Ishikawa, A., Kobayashi, H., Tsuhara, Y., Kawashima, M., Suzuki, K., Muto, S., and Matsui, M. (2003). Activation tagging, a novel tool to dissect the functions of a gene family. Plant J. **34,** 741–750.

Nemhauser, J.L., Feldman, L.J., and Zambryski, P.C. (2000). Auxin and *ETTIN* in *Arabidopsis* gynoecium morphogenesis. Development **127,** 3877–3888.

Ni, M., Tepperman, J.M., and Quail, P.H. (1998). PIF3, a phytochrome-interacting factor necessary for normal photoinduced signal transduction, is a novel basic helix-loop-helix protein. Cell **95,** 657–667.

Ouellet, F., Overvoorde, P.J., and Theologis, A. (2001). IAA17/AXR3: Biochemical insight into an auxin mutant phenotype. Plant Cell **13,** 829–841.

Page, R.D. (1996). TreeView: An application to display phylogenetic trees on personal computers. Comput. Appl. Biosci. **12,** 357–358.

Parenicova, L., De Folter, S., Kieffer, M., Horner, D.S., Favalli, C., Busscher, J., Cook, H.E., Ingram, R.M., Kater, M.M., Davies, B., Angenent, G.C., and Colombo, L. (2003). Molecular and phylogenetic analyses of the complete MADS-box transcription factor family in Arabidopsis: New openings to the MADS world. Plant Cell **15,** 1538–1551.

Pinyopich, A., Ditta, G.S., Savidge, B., Liljegren, S.J., Baumann, E., Wisman, E., and Yanofsky, M.F. (2003). Assessing the redundancy of MADS-box genes during carpel and ovule development. Nature **424,** 85–88.

Redman, J.C., Haas, B.J., Tanimoto, G., and Town, C.D. (2004). Development and evaluation of an Arabidopsis whole genome Affymetrix probe array. Plant J. **38,** 545–561.

Reed, J.W. (2001). Roles and activities of Aux/IAA proteins in Arabidopsis. Trends Plant Sci. **6,** 420–425.

Remington, D.L., Vision, T.J., Guilfoyle, T.J., and Reed, J.W. (2004). Contrasting modes of diversification in the *Aux/IAA* and *ARF* gene families. Plant Physiol. **135,** 1738–1752.

Ren, B., et al. (2000). Genome-wide location and function of DNA binding proteins. Science **290,** 2306–2309.

Rogg, L.E., Lasswell, J., and Bartel, B. (2001). A gain-of-function mutation in *IAA28* suppresses lateral root development. Plant Cell **13,** 465–480.

Rouse, D., Mackay, P., Stirnberg, P., Estelle, M., and Leyser, O. (1998). Changes in auxin response from mutations in an AUX/IAA gene. Science **279,** 1371–1373.

Sambrook, J., Fritsch, E.F., and Maniatis, T. (1989). Molecular Cloning: A Laboratory Manual, 2nd Ed. (Cold Spring Harbor, NY: Cold Spring Harbor Laboratory Press).

Sessions, A., et al. (2002). A high-throughput Arabidopsis reverse genetics system. Plant Cell **14,** 2985–2994.

Sessions, A., Nemhauser, J.L., McColl, A., Roe, J.L., Feldmann, K.A., and Zambryski, P.C. (1997). *ETTIN* patterns the *Arabidopsis* floral meristem and reproductive organs. Development **124,** 4481–4491.

Sessions, R.A., and Zambryski, P.C. (1995). *Arabidopsis* gynoecium structure in the wild and in ettin mutants. Development **121,** 1519–1532.

Shuai, B., Reynaga-Pena, C.G., and Springer, P.S. (2002). The lateral organ boundaries gene defines a novel, plant-specific gene family. Plant Physiol. **129,** 747–761.

Smith, D.L., and Fedoroff, N.V. (1995). *LRP1*, a gene expressed in lateral and adventitious root primordia of Arabidopsis. Plant Cell **7,** 735–745.

Staswick, P.E., Tiryaki, I., and Rowe, M.L. (2002). Jasmonate Response Locus *JAR1* and several related Arabidopsis genes encode enzymes of the firefly luciferase superfamily that show activity on jasmonic, salicylic, and indole-3-acetic acids in an assay for adenylation. Plant Cell **14,** 1405–1415.

Stowe-Evans, E.L., Harper, R.M., Motchoulski, A.V., and Liscum, E. (1998). NPH4, a conditional modulator of auxin-dependent differential growth responses in Arabidopsis. Plant Physiol. **118,** 1265–1275.

Tatematsu, K., Kumagai, S., Muto, H., Sato, A., Watahiki, M.K., Harper, R.M., Liscum, E., and Yamamoto, K.T. (2004). *MASSUGU2* encodes Aux/IAA19, an auxin-regulated protein that functions together with the transcriptional activator NPH4/ARF7 to regulate differential growth responses of hypocotyl and formation of lateral roots in *Arabidopsis thaliana*. Plant Cell **16,** 379–393.

Thompson, J.D., Higgins, D.G., and Gibson, T.J. (1994). CLUSTAL W: Improving the sensitivity of progressive multiple sequence alignment through sequence weighting, position-specific gap penalties and weight matrix choice. Nucleic Acids Res. **22,** 4673–4680.

Tian, C., Muto, H., Higuchi, M., Matamura, T., Tatematsu, K., Koshiba, T., and Yamamoto, K.T. (2004). Disruption and overexpression of auxin response factor 8 gene of Arabidopsis affect hypocotyl elongation and root growth habit, indicating its possible involvement in auxin homeostasis in light condition. Plant J. **40,** 333–343.

Tian, Q., and Reed, J.W. (1999). Control of auxin-regulated root development by the *Arabidopsis thaliana SHY2/IAA3* gene. Development **126,** 711–721.

Tian, Q., Uhlir, N.J., and Reed, J.W. (2002). Arabidopsis SHY2/IAA3 inhibits auxin-regulated gene expression. Plant Cell **14,** 301–319.

Tiwari, S.B., Hagen, G., and Guilfoyle, T. (2003). The roles of auxin response factor domains in auxin-responsive transcription. Plant Cell **15,** 533–543.

Tiwari, S.B., Hagen, G., and Guilfoyle, T.J. (2004). Aux/IAA proteins contain a potent transcriptional repression domain. Plant Cell **16,** 533–543.

Tsuchisaka, A., and Theologis, A. (2004). Heterodimeric interactions among the 1-amino-cyclopropane-1-carboxylate synthase polypeptides encoded by the Arabidopsis gene family. Proc. Natl. Acad. Sci. USA **101,** 2275–2280.

Ullah, H., Chen, J.G., Temple, B., Boyes, D.C., Alonso, J.M., Davis, K.R., Ecker, J.R., and Jones, A.M. (2003). The β-subunit of the Arabidopsis G protein negatively regulates auxin-induced cell division and affects multiple developmental processes. Plant Cell **15,** 393–409.

Ulmasov, T., Hagen, G., and Guilfoyle, T.J. (1997). ARF1, a transcription factor that binds to auxin response elements. Science **276,** 1865–1868.

Ulmasov, T., Hagen, G., and Guilfoyle, T.J. (1999a). Dimerization and DNA binding of auxin response factors. Plant J. **19,** 309–319.

Ulmasov, T., Hagen, G., and Guilfoyle, T.J. (1999b). Activation and repression of transcription by auxin-response factors. Proc. Natl. Acad. Sci. USA **96,** 5844–5849.

Vogler, H., and Kuhlemeier, C. (2003). Simple hormones but complex signalling. Curr. Opin. Plant Biol. **6,** 51–56.

Ward, S.P., and Estelle, M. (2001). Auxin signaling involves regulated protein degradation by the ubiqutin-proteasome pathway. J. Plant Growth Regul. **20,** 265–273.

Watahiki, M.K., and Yamamoto, K.T. (1997). The massugu1 mutation of Arabidopsis identified with failure of auxin-induced growth curvature of hypocotyl confers auxin insensitivity to hypocotyl and leaf. Plant Physiol. **115,** 419–426.

Worley, C.K., Zenser, N., Ramos, J., Rouse, D., Leyser, O., Theologis, A., and Callis, J. (2000). Degradation of Aux/IAA proteins is essential for normal auxin signalling. Plant J. **21,** 553–562.

Yang, T., and Poovaiah, B.W. (2000). Molecular and biochemical evidence for the involvement of calcium/calmodulin in auxin action. J. Biol. Chem. **275,** 3137–3143.